CHALMERS
UNIVERSITY OF TECHNOLOGY

Simulation of Charge Dynamics in Oil-Cellulose Insulation

Master's thesis in Electrical Engineering

DANIEL AHLQVIST

DEPARTMENT OF ELECTRICAL ENGINEERING

CHALMERS UNIVERSITY OF TECHNOLOGY
Gothenburg, Sweden 2022
www.chalmers.se

Master Thesis 2022

Simulation of charge dynamics in oil-cellulose insulation

DANIEL AHLQVIST

Division of Electric Power Engineering
Department of Electrical Engineering
Chalmers University of Technology
Gothenburg, Sweden 2022

Simulation of charge dynamics in oil-cellulose insulation
Daniel Ahlqvist

Examinator: Yuriy Serdyuk, Department of Electric Power Engineering
Supervisor: Olof Hjortstam, Hitachi Power Grids Research

Master Thesis
Institution of Electric Power Engineering
Division of Electrical Engineering Chalmers University of Technology
412 96 Göteborg
Telefon +46 31 772 1000

Typeset in LaTeX
Gothenburg, Sweden 2022

Simulation of charge dynamics in oil-cellulose insulation

DANIEL AHLQVIST
Division of Electric Power Engineering
Department of Electrical Engineering
Chalmers University of Technology

Abstract

The rise of the energy demand and trends in increasing distances between power plants and energy consumption locations have increased the need for highly efficient power transfer. This has led to the rise in usage of High Voltage Direct Current (HVDC) transmission due to its superior efficiency for long distances. One key component of this system is the HVDC converter transformer. The electrical insulation of HVDC converter transformers is normally made of mineral oil and oil-impregnated pressboard. It is exposed to extremely high combined AC and DC voltage, which activate transport of electrical charges in the materials and their accumulation on materials interfaces. The latter causes hardly predictable modifications on electric field in the insulation, which needs to be properly designed to withstand local field enhancements and to provide continuous operation of the transformer. The aim of the present study is to implement and to test a computational tool for simulations of charge dynamics and associated electric fields in oil-pressboard insulation system.

A model based on partial differential equations describing physical processes of generation, losses and transport of charged species (ions) in transformer oil and oil-impregnated pressboard has been developed. It is assumed that ions are generated due to field-enhanced dissociation of oil molecules in the oil bulk and at the electrodes (the latter is considered as apparent injection) and they may be neutralized due to recombination and surface reactions. Drift of ions through the material is controlled by the local electric field and is defined by respective electric ionic mobility. The resulted model comprised so-called drift-diffusion-reaction equations for concentrations of ions in the materials coupled with Poisson's equation for the electric potential and it was implemented in COMSOL Multiphysics. The model has been verified by conducting simulations for several study cases and comparing the results with published data.
The influences of the different physical properties on charge transport in the insulation have been studied using the developed computer model. Thus, a set of simulations have been performed to analyze the effects of the mobilities of ions (in particular, their field dependencies) and the intensity of injection of ions into pressboard, on the dynamic behavior of the electric field in oil-pressboard system. From this study, it can be concluded that charge accumulation is mainly affected by the differences in the mobilities of positive and negative ions, while the effect of their field dependences is rather minor. Furthermore, the ion generation rate inside the pressboard contributes the most to the charging and increases with the electric field.

Keywords— HVDC Insulation, Power Transformer Insulation, HVDC concerter, Oil-Impregnated Pressboard, electric conductivity, Ion Drift Model, Ion Mobility.

Acknowledgements

I would like to show my most sincere appreciation for my supervisor, Adjunct Professor Olof Hjortstam, for providing crucial support during the whole project. Olof introduced the topic, patiently helped me build up a good framework and offered advice with pinpoint accuracy.

I also want to highlight my examiner, Professor Yuriy Serdyuk. With the help at short notice and his great expertise in COMSOL, Yuriy always offered and shared his knowledge to help overcome obstacles which could have prolonged this thesis significantly. Together with Olof, without them this work would not have been possible.

A special thanks also goes out to Joachim Schliessling at Hitachi Energy Research, for providing help and knowledge from a more practical and laboratory view. This has been helpful to give this project a more stable ground outside the theoretical part.

Finally I want to thank my family and friends, who have provided support and understanding that have helped me put down the time needed for this thesis to be completed.

Daniel Ahlqvist, June 2022

Contents

List of Figures

List of Tables

1
Introduction

This thesis is part of a collaboration between Hitachi Energy Research and Chalmers University of Technology. This chapter introduces the background of the project, the aim and the objectives of the thesis. It also handles the limitations of the thesis and the structure of the report.

1.1 Background

With the increase in energy demand all over the world and the increase in renewable energy output, the places where the power plants are being built have increased the distance between the power plant and the people needing the power. For example, many of the wind farms are being constructed out in open water. This leads to the need for power transfer that can compensate for the longer transfer distance by having a higher efficiency. High Voltage Direct Current is more efficient over long distances than the AC-system and can transport power in cables under water without high losses. Before it was an expensive technology, which has become more affordable due to the increase in knowledge and better construction techniques. One important part of the HVDC power grid is the HVDC converter stations that are required to convert the voltage between high AC and high DC voltage. These consist of DC-converters and also include a power transformer. This power transformer is subjected to a combined AC/DC stress. This puts a lot of importance on their insulation system, which needs to be able to withstand both DC and AC stress. The most common insulator for power transformers in the world is the oil-impregnated pressboard (or paper) insulation, consisting of a cellulose solid which has been impregnated with transformer oil [1]. It is an old technology, which is still in need of much research to understand its behavior in DC electric fields and what processes are in work inside the bulk of the pressboard during stresses from electric fields. The transformer oil is well understood how it works [2],[3] and the composition of the pressboard itself is well known, those two combined creates theoretical and practical questions how they work together.

1.2 Aim of the Thesis

This thesis will take a look at some of the processes inside the pressboard and see what effect the electric field has on them. It will look at the possible effect of field dependent ionization, field dependent injection, field dependent mobility of ions and combinations of these with the help of Ion Drift Conduction modeling. This will then be compared to laboratory results to determine if the Ion Drift model gives similar results and which factors are field dependent and affect the space charge density. When either the results

using the model lines up with the laboratory or a stop due to limitations has been reached, the thesis can be defined as completed.

1.3 Objectives

To achieve the aim state above, several parts needs to be completed.

- Implement the Ion Drift Conduction model using the most current version of COMSOL Multiphysics.
- Recreate the results from earlier simulations to verify that the model is working correctly.
- Simulate the effect of contact resistivity to be able to recreate this in later simulations.
- Adapt the model for a pure, pressboard model with the ability to implement field dependent ionization, injection and mobility.
- Find earlier parameters and spatial resolutions that can be used in the simulations to achieve results that can be compared with laboratory results.
- Simulate a test based on Pulsed Electro Acoustics (PEA) laboratory results [4] to test which of the three above factors does impact the space charge density inside the pressboard.
- If needed, modify the parameters to achieve the same results as the laboratory PEA results.

To help calculate the processes, the ion-drift diffusion conduction model will be used with the help of COMSOL Multiphysics. The Ion Drift model is dependent on the relative permittivity, conductivity and the mobilities of positive and negative ions inside the simulated sample, which it uses to simulate the processes inside the sample [1]. This model will simulate the results of Pulsed Electro Acoustic laboratory results and see what processes inside the pressboard are dependent on the electric field. The test sample that will be simulated is a simplified version of a test sample with a pressboard surrounded by epoxy.

1.4 Limitations

The mesh used in the simulations will give different results for different mesh sizes. This needs to be taken into consideration when simulating earlier work, so that the correct mesh size is in use when trying to replicate earlier results.
The effect of the temperature on the material will not be considered in the following simulations, so all simulations will be defined to be at room temperature. Due to the effect of electric field, resistivity and other factors, this will limit the amount of work needed to be performed while also limiting the accuracy of the simulations when the property is dependent on temperature.
Some results are not known from earlier laboratory results, therefore similar results will need to be found to find parameters that can replicate the desirable results. Some physical aspects will need to be theoretically calculated, which may lead to different results than the

laboratory results. For example, the contact resistance will be calculated by simplification and taken from earlier work. This might affect the electric field over simulated samples, reducing the accuracy of the work.
The effect of the diffusion will not be completely simulated, this to decrease the workload and simplify the approach.

1.5 Structure of the Report

This report is divided into five parts, with Introduction being the first part. Chapter two deals with the theory around Ion Drift, contact resistivity and field dependency of mobility. Chapter three introduces the computer model and the materials, plus the different parts that will be important. Chapter four shows the results of different simulations, from start to a more finished result. Chapter five discusses the results and the different factors that affect the results, while also adding how the oil-impregnated pressboard will have a place in a sustainable future. Chapter six concludes everything and introduces possible future work.

2
Physical Model

2.1 Ion-drift Model

To calculate the ionization, recombination, diffusion and movement of ions in weak electrolytes, there are different methods that can be used to simulate it or measure it in laboratories. Some of these include the *RC-model* [1], the *Pulsed Electro Acoustic method* (PEA) [5], the *Electro-optic Kerr Method* [1] and the *Ion Drift Diffusion model* [1]. In this report, the focus will be on the *Ion Drift Diffusion model* and try to replicate results of PEA-measurements in [4].

2.1.1 Charge Carriers in Transformer Oil

The ion drift model is a model that is used to describe oil and its properties during DC voltage stress, for which it has been proven to be an useful model [1]. It is a fairly simple model, using four parameters that are relatively easy to measure. These are resistivity, relative permittivity and the mobility of both negative and positive ions. These are measured during low voltage and the results can be used to estimate the behavior of oil at much higher voltages, making it practical to use when estimating the behavior of transformer oil when it is affected by the DC voltage in HV products such as HVDC converter transformers.
Transformer oil is an insulating liquid used in transformers and is considered a weak electrolyte by the ion drift model [6]. Its resistivity is dependent on the amount of free charges (negative and positive ions) present, which increases when affected by an high external electric field or by elevated temperature. Due to this, the equilibrium between the density of ionic pairs (neutral molecules) c and the densities of positive and negative ions, p and n, is not static. Ionic pairs are formed by the recombination of ions, while free ions are generated from dissociation of ionic pairs [1]. Electric conduction of the oil is then dependent on the ions in the liquid (residual conduction) or due to injected charges coming from the electrodes (injection) [7]. The rate of which the dissociation and recombination of ions is given by the rate equation [6]:

$$\frac{dp}{dt} = \frac{dn}{dt} = k_D c - k_R p n \tag{2.1}$$

Here k_D represents the dissociation constant while k_R represents the recombination constant. For non-polar liquids, density of ionic pairs c can be taken as a constant, while the concentrations p and n satisfy the conditions $p << c$ and $n << c$.
If the electrical mobilities of the positive and negative ions are known, μ_p and μ_n, the recombination constant in 2.1 can be obtained using Langevin approximation:

$$k_R = \frac{q(\mu_p + \mu_n)}{\epsilon_0 \epsilon_r} \tag{2.2}$$

Here ϵ_0 is the permittivity of vacuum and ϵ_r is the permittivity of the transformer oil. From this equation, it can be noted that it is not dependent on the electric field. Therefore it will occur at the same rate at any time.
According to Onsager's theory [8], this is not the case for the dissociation constant, which is a function of the electric field

$$k_D = k_D^0 F(b) = k_D^0 \frac{I_1(4b)}{2b} \tag{2.3}$$

Here I_1 is the modified Bessel function of first kind and order. The electric field strength is considered in the term b as:

$$b = \frac{L_B}{L_E} = \sqrt{\frac{q^3|E|}{16\pi\epsilon_0\epsilon_r k^2 T^2}} \tag{2.4}$$

Here T is the temperature, k is the Boltzmann constant and q is the elementary charge. The distance $L_B = q^2/8\pi\epsilon_0\epsilon_r kT$ is known as the Bjerrum distance. This refers to the approximate distance within which electrostatic interactions dominate thermal motions for two charges. From this, it can be concluded that the thermal energy kT is half of the electrostatic energy corresponding to two ions of opposite signs at distance L_B. Concurring with this, the force exerted by the external field E equals the mutual force between the same ions separated at a distance $L_E = (q/4\pi\epsilon_0\epsilon_r|E|)^{1/2}$. In the limit $E \to 0$, b goes to zero and the dissociation constant 2.3 has the constant value k_D^0 due to $F(b) \to 1$.
When at thermodynamic equilibrium (absence of external electric field), the densities of positive and negative ions are identical and constant, $p = n = n_0$ in the bulk of the fluid. From 2.1, the ratio between the dissociation and recombination constants in this equilibrium is

$$\frac{k_R}{k_D^0} = \frac{c}{n_0^2} \tag{2.5}$$

and the equilibrium density of the charge carriers can be found by using the resistivity of the liquid

$$n_0 = \frac{\sigma}{q(\mu_p + \mu_n)} \tag{2.6}$$

Here q is the elementary charge, σ is the conductivity and μ_p and μ_n are the mobilities of the positive and negative ions respectively. If there is an external electric field applied, the equilibrium conditions of 2.5 and 2.6 are no longer valid.
Due to the electric field, charge carriers in the bulk of the fluid will start to drift towards the electrode with opposite signs due to being subjected to electrostatic forces. The velocity that the charge carriers drift with is defined by their mobilities and the strength of the electric field.

$$\vec{w}_{p,n} = \mu_{p,n}\vec{E} \tag{2.7}$$

This leads to differences in concentrations of ions in different points in space, which causes diffusion of charge carriers. The diffusive fluxes have magnitudes that are proportional to the gradients of the ion's densities, $-D_p\nabla_p$ for positive and $-D_n\nabla_n$ for negative. Using Einstein's relation [6], the diffusion coefficients $D_{p,n}$ are found:

$$D_{p,n} = \frac{kT}{q}\mu_{p,n} \tag{2.8}$$

Taking into account the drift 2.7 and diffusion 2.8 the rate equation 2.1 can be extended to equations describing the transport of charges through the bulk of a fluid while accounting

for sources and sink of charges. These are called the continuity equations.

$$\frac{\partial p}{\partial t} + \nabla(\mu_p \vec{E} p - D_p \nabla p) = k_D^0 c F(E) - k_r p n \tag{2.9a}$$

$$\frac{\partial n}{\partial t} - \nabla(\mu_n \vec{E} n + D_n \nabla n) = k_D^0 c F(E) - k_r p n \tag{2.9b}$$

The ionic current between two electrodes can be defined by the total ionic fluxes:

$$\vec{j}_p = q(\mu_p \vec{E} p - D_p \nabla p), \vec{j}_n = -q(\mu_n \vec{E} n + D_n \nabla p), \vec{j}_{tot} = \vec{j}_p + \vec{j}_n \tag{2.10}$$

By integrating the current density $\vec{j}_{tot}$, the total current in the external circuit can be found. The transport of charge equations 2.9 contains coefficients that are dependent on the field. These should be supplemented by Poisson's equation for the electrical potential ϕ in order to obtain the electric field distribution that is affected by the space charge in the system

$$\nabla(\epsilon_0 \epsilon_r \nabla \phi) = -q(p - n), \vec{E} = -\nabla \phi \tag{2.11}$$

Here, the electric potential is the function of space coordinates $\phi = \phi(x, y, z)$ with known magnitudes on the boundaries, in this model the electrodes or walls. The above equations describes the processes that are in the bulk of the fluid. The phenomena at boundaries, such as interfaces between oil and metal, are characterized by a preferential absorption of one kind of ions with the sign which is opposite to the polarity of the metallic surface. These ions are diffusively distributed over a thin boundary region that is called an electrical double layer, whose thickness λ is essentially the Debye length. This is calculated as:

$$\lambda = \sqrt{D \epsilon_0 \epsilon_r / \sigma} \tag{2.12}$$

In transformer oil, the typical magnitude of λ is in the order of tenths of micrometers. More in depth analysis of the electrical double layer is to be found in chapter 2.2.1. Due to the preferential absorption, there is an injection of charges having the same sign as the boundary into the bulk of the fluid. This apparent injection of charges can be seen as a three step process [7]: (i) in the vicinity of an electrode, ionic pairs are attached at the metal surface by the electrostatic image force; (ii) charge transfer reactions occur between the metal and ionic pairs, which leads to reduction or oxidation of the ions constituting the ionic pair and dissociation of the ionic pairs; (iii) extraction of the other ion of the ionic pair from the interface by the Schottky effect. This leads to the injected carriers being identical to the corresponding ions created by the dissociation in the bulk of the fluid. The density of the apparent injected charges due to the escape of ions from the double layer due to the Schottky effect can be described as [7]

$$n_{inj} = n_0 F_i(b) = \frac{n_0}{2bK_1(2b)} \tag{2.13}$$

Here K_1 is the modified Bessel function of the second kind and first order, while argument b is to be evaluated at the injecting surface which is dependent on the electric field. The field enhancement of injection is weaker than the dissociation of oil molecules and are only comparable in the low field region, i.e. in the range $E < 2 * 10^6 V/m$. Therefore it can be expected that the injection of ions at a metallic surface can contribute significantly to the total rate of generation of ions in two cases: (i) when the magnitude of the field in the vicinity of the electrode is in the indicated range, and (ii) when the amount of ions are lowered in the bulk of the fluid due to the sweep-out effect. These situations are

considered in the following sections. By taking the equilibrium density of charge carriers from equation 2.6 into account, the injected charge can be shown to be related to the conductivity of the fluid:

$$n_{inj} = \frac{\sigma}{q(\mu_p + \mu_n) * 2bK_i(2b)} \tag{2.14}$$

From there, by knowing the density of the injected charges, the injected current can be defined as:

$$\vec{j}_{inj} = q\mu n_{inj}\vec{E}_{sur} \tag{2.15}$$

Here, E_{sur} is the electric field at the injecting surface, while μ is the mobility of either the negative or the positive charges, depending on the sign of the potential that is applied to the injecting surface. The total current density in general is the result of the positive and negative charge ions.

$$J_{total} = J_n + J_p \tag{2.16}$$

Its velocity is the same as 2.7 and its current is the same as 2.15, modifying it to include the concentration of negative and positive ions.

$$\vec{J} = q\vec{E}(n\mu_n + p\mu_p) \tag{2.17}$$

If $p = n$, then 2.17 is the same as 2.15 for the non-injected concentrations. The amount of space charges is also needed, which is dependent on the amount of negative and positive charges:

$$\rho = q(p - n) \tag{2.18}$$

2.1.2 Charge Carriers in Oil Impregnated Pressboard

Oil impregnated pressboard is a common insulator used in transformers. These consist of pressboard that have been impregnated with oil, which enhances their insulating properties. They can therefore be considered as composite structures consisting of a cellulose-fiber matrix with pores filled with oil, which the internal arrangement is very complex. In basic, the structural components of the pressboard are long cellulose fibers that are approximately cylindrical in shape. Each fiber is a composite of dense fibril aggregates that is formed of large molecules of cellulose. The length of these fibers may be up to several millimeters, while the width is around $30\mu m$. The fibers are also interlaced with one another to form a quite dense microstructure with the spacing between fibers ranging between $3 - 10\mu m$. These capillary channels, that are formed by cellulose, are filled with oil during the impregnation process.
The difference in charge generation and transport process are different for oil and pressboard, which makes the process vary depending on where in the material it is occuring. If an external field is applied, charges in the bulk of the impregnated pressboard may appear due to several reasons: result of de-trapping from surface traps on cellulose fiber, generated on the oil phase inside the microstructures due to field enhancement dissociation, and being injected through the interfaces between the impregnated board (from the oil side) and the core oil. Occurring simultaneously, recombination and trapping induces losses of free charges. The charge carriers in the bulk of the impregnated pressboard are transported through the material due to electric forces, whose direction is dependent on the electric field.
Using apparent effective (averaged) values for kinetic and rate coefficients, the charge transport in an oil-impregnated pressboard can be described using the basis from the ion-drift model from chapter 2.1.1. This leads to the need to obtain these coefficients

from measurements obtained experimentally, such as space charge dynamics (which yields mobilities) and conductivity (that yields the equilibrium concentration of charges). The permittivity of the oil-pressboard structure is found using an average approach: with permittivity of oil at around 2.2 while cellulose fiber are around 6-7, depending on the density. This results in a permittivity of around 3.4 to 4.5 for the mixed dielectric [9]. This allows simplification of the model if the processes in the bulk of the impregnated pressboard do not need a detailed analysis.

2.1.3 Behavior at interfaces

As mentioned in chapter 2.1.1 (and in more detail in 2.2.1), the drifting and separation of charges generated due to the applied field leads to the formation of double layers close to the oil-electrode interface. A similar process occurs when the ions meet a solid dielectric surface while drifting towards the opposite-charged electrode. In this case, ions are able to penetrate partially into the bulk of the material where they are subjected to different conditions than in the oil. The pressboard therefore affects the mobility and characteristic diffusion length of the ions, lowering their magnitude significantly. This leads to a charge relaxation with a characteristic time constant in the range 1-100 seconds at the interfaces [10].

2.2 Resistivity of contacts

Here the concept of contact resistivity is discussed. This will be used to calculate the decrease in voltage due to resistance in the materials next to the test sample. In the simulations, it will be defined as a voltage drop. The concept of electrical double layer and the concept of the contact resistivity will be discussed.

2.2.1 Electrical double layer

At the borders between different materials, such as between oil and the electrode or the oil and the pressboard, the concentration of ions will vary depending on the mobility and the polarity of the boundary. At the boundary between oil and the electrode, there will be a higher concentration of ions of the kind that is reversible to the polarity of the electrode, as mentioned in chapter 2.1. Two different layers will form at the boundary, which has given the name of the electrical double layer. The layer closest to the electrode is called the surface layer, which is made up by the ions that are attached to the electrode surface directly due to polarity. Negative ions will accumulate at the positive electrode, while positive ions will accumulate at the negative electrode. The second layer is named the diffuse layer, which is composed of ions that are loosely bound to the surface layer. These are attracted by the polarity, which is governed by the Coulomb force. From equation 2.17, it is known that the amount of ions and the magnitude of the electric field will contribute to a higher current. Due to this, the concentration close to the electrode will affect the electric field.

2.2.2 Contact Resistance

The voltage that the material is subjected to is not just dependent on the voltage that is applied, but also the voltage drop that occurs near the electrode

$$V_{app} = V_{oil} + \Delta V_1 + \Delta V_2 \tag{2.19}$$

Here ΔV_n is the voltage drop due to the contact resistivity that is formed due to the electrical double layer. To be able to calculate the resistivity of the contacts, the current and the resistivity is needed.

$$2 * \Delta V_n = J \rho l_c \tag{2.20}$$

Here l_l is the thickness of the double layer. Conductivity and resistivity have an inverse relationship, which may be used to calculate the other.

$$\sigma = \frac{1}{\rho} \tag{2.21}$$

Using this and modifying equation 2.6, a equation where the concentrations are dependent on the resistivity can be found

$$n = p = \frac{1}{q\rho(\mu_p + \mu_n)} \tag{2.22}$$

To be able to calculate the contact resistance, the relationship between resistance and resistivity is needed. This is dependent on the area of the electrodes and the distance between them, in between there is a material that will give rise to the contact resistance between the electrode and the material.

$$R = \rho \frac{d}{A} \tag{2.23}$$

Here A is the area of the electrode and d is the distance between two flat electrodes. For the contact resistance, the distance is small and this equation may not be sufficient to calculate the contact resistance. Another way is to combine 2.23 with the equation of the geometric capacitance.

$$C_0 = \epsilon_0 \epsilon_r \frac{A}{d} \tag{2.24}$$

Here ϵ_0 is the permittivity of vacuum and ϵ_r is the permittivity of the material in between the electrodes. When calculating the geometric capacitance value, it is assumed to be vacuum between the electrodes, therefore removing the permittivity of the material leaving the permittivity of vacuum. Combining 2.23 and 2.24 gives

$$R = \rho \frac{\epsilon_0}{C_0} \tag{2.25}$$

This resistance is a combination of multiple resistances.

$$R = R_{electrode,1} + R_{Contact,1} + R_{material} + R_{Contact,2} + R_{electrode,2} \tag{2.26}$$

The resistance of the electrode is mostly insignificant, since its purpose is to conduct effectively. Therefore 2.26 can be rewritten as

$$R = 2R_{Contact} + R_{material} \tag{2.27}$$

If the resistance of the material is known, then the contact resistance can be calculated. Due to time constraints, the contact resistance was not implemented and explored in model used for this Master Thesis work. The theoretical formulations is however included as input for future work on this topic.

2.3 Mobility dependency on the Electric Field

As mentioned in chapter 2.1, there are different methods that can be used when calculating and measuring ionization, recombination, diffusion and movements of ions in weak electrolytes. One of the methods mentioned was the *Pulsed Electro Acoustics*, or *PEA*. It is a common method that is often used in laboratories. The measurements using the PEA method are made by generating moving charges that produces acoustics waves in the material by using high frequency voltage. The measurements are therefore dependent on the permittivity and conductivity of the materials, while also needing the acoustic impedance (measured in NS/m^3) of the material. The method has been used to try to calculate the dependency of mobility on the electric field in [4] by encapsuling a oil-impregnated pressboard with a blocking layer made of epoxy. To be able to do similar calculations with the Ion drift model, the equations in chapter 2.1 needs to be modified.

Equation 2.17 can be defined as the transport equation, while equation 2.18 can be rewritten as:

$$\epsilon \frac{\partial E(x,t)}{\partial x} = \rho(x,t) \tag{2.28}$$

¨ which is the Poisson equation. Adding the continuity equation

$$\frac{\partial J(x,t)}{\partial x} + \frac{\partial \rho(x,t)}{\partial t} = S \tag{2.29}$$

where S is the source term which includes trapping, detrapping, recombination and ionization, these three equations can be used to describe the migration process inside an insulation material. If the involvement of the trapping, detrapping, recombination and ionization can be added to the mobility, the source term becomes zero. This is a crude approximation that is used in [5] that does not resolve the details in the physics as well as the full Ion-Drift model in chapter 2.1. Using equation 2.17, the average current in the test sample can be described as

$$J_{avg}(t) = \frac{\mu}{d_2} \int_{d_1}^{d_1+d_2} \rho(x,t) E(x,t) dx \tag{2.30}$$

where $d_2 - d_1$ is the thickness of the test sample. The space charge density $\rho(x,t)$ can be divided into two parts, the interface between the blocking layer (epoxy in [4]) and the test sample and the charges inside the bulk of the test sample. This leads to the total amount of charges expression to be written as

$$Q(t) = \int_{d_{start}}^{d_{end}} \rho(x,t) dx + \int_{d_{end}}^{d_1+d_2} \rho(x,t) dx \tag{2.31}$$

where d_{start} and d_{end} are the start and end points of the interface charges measured. The first term is the interface charges, while the second is the bulk charges. To simplify the calculations, the local field distributions are simplified to an average electric field which is calculated using

$$E_{avg}(t) = \frac{1}{d_2} \int_{d_1}^{d_1+d_2} \left(\frac{Q_0(t) + Q_{io}(t)}{\epsilon_1} + \int_{d_1}^{x} \frac{\rho_{io}(x,t)}{\epsilon_2} d\delta \right) dx \tag{2.32}$$

$Q_0(t)$ is the induced charge at the cathode

$$Q_0(t) = \int_{d_{01}}^{d_{02}} \rho(x,t) dx \tag{2.33}$$

while d_{01} and d_{02} are the start and end points of the measured induced charge at the cathode. This simplification will be used and discussed later in this report. Adding equation 2.32 into 2.30 gives:

$$J_{avg}(t) = \frac{\mu E_{avg}(t)}{d_2} \int_{d_1}^{d_1+d_2} \rho(x,t)dx \tag{2.34}$$

Using equation 2.34 and 2.31, the apparent mobility of the carrier, which includes lumped behavior from equation 2.29, can be described as

$$\mu = \frac{d_2 J_{avg}(t)}{Q(t)E_{avg}(t)} \tag{2.35}$$

With the source term being zero, 2.29 can be rewritten as

$$J(t) = \int \frac{d\rho(x,t)}{dt}dx = \frac{d(\int \rho(x,t)dx)}{dt} \tag{2.36}$$

The current density at the interface can be used to approximately characterize the current density in the test sample. If used, this gives the average current density as

$$J_{avg}(t) = \frac{d(\int_{d_{start}}^{d_{end}} \rho(x,t)dx)}{dt} = \frac{dQ_{if}(t)}{dt} \tag{2.37}$$

Finally equation 2.35 can be rewritten

$$\mu = \frac{d_2 \frac{Q_{if}(t)}{dt}}{Q(t)E_{avg}(t)} \tag{2.38}$$

The equation can be more intricate by reducing the effect of ionization on the mobility. This is not needed in this report, due to the focus being on all field dependent factors.

3
Implementation of Model

In this chapter, the implementation of the problems will be discussed. The implementation is done using COMSOL Multiphysics v. 6.0, a useful tool to simulate electric phenomenons and to combine it with the physics that occur in liquids and solids. The model in this report is simulating a gap between two electrodes, in which a sample of oil-impregnated pressboard surrounded by epoxy has been put. This can be accomplished in different ways, where a 3D model or a 2D model would work well. The physics used in this model can be simplified to a 1D model, which is the one that will be used here.

3.1 Geometry and Materials

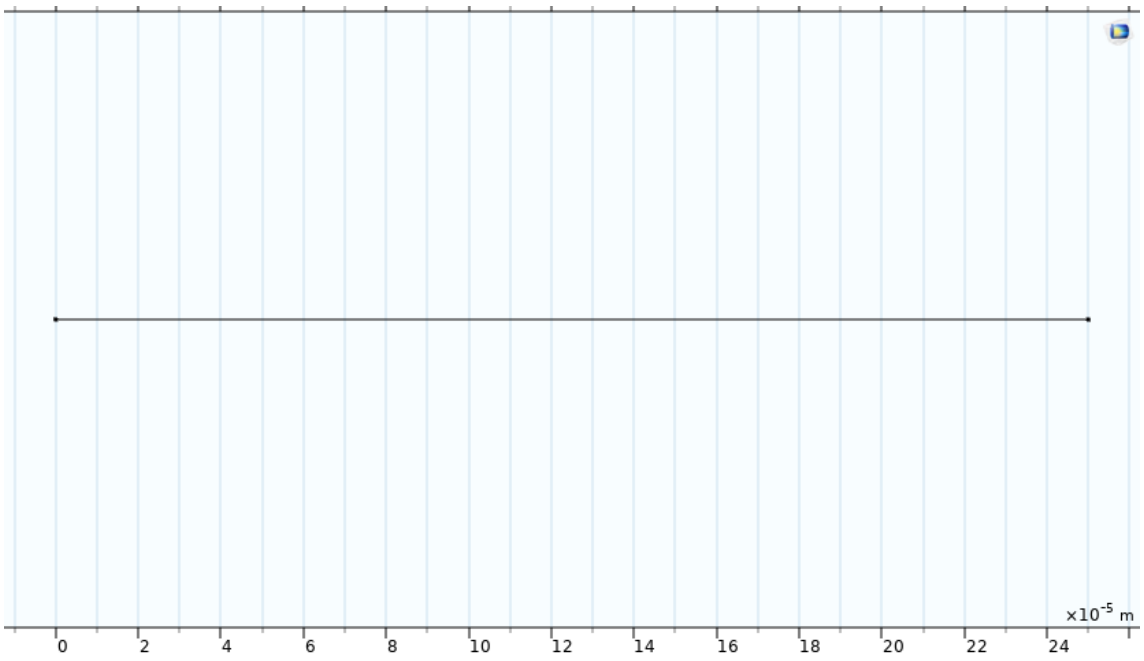

Figure 3.1: Pressboard 1D model

The properties of the oil-impregnates pressboard will be discussed in 3.3. The model is designed in a 1D plane geometry, using intervals to simulate the different parts of the gap between the electrodes. The electrodes are only defined as the boundary at the ends, since their effect on resistance and resistivity is negligible. The model for the pressboard and epoxy gap is defined by the PEA measurements used in earlier research [4]. This model is simplified by having a single interval, which length is 250 μm, which only consists of

the pressboard itself. The epoxy's impact on the model is simulated without having the epoxy as separate intervals. How this is done is defined in 3.2.2. The model can be seen in figure 3.1

3.2 Multiphysics needed

To simulate an electric field affecting the model, the equations from chapter 2.1.1 needs to be fulfilled. To be able to do this, COMSOL uses physics that are used to implement and compute the different physical aspects of the model. This model will need to compute the electric fields, the polarities of DC-Voltage and the ionic charge dynamics happening in the oil and the pressboard. Due to the diffusion and ion-drift occurring when the model is subjected to an electric field, the solution needs to be over time. Therefore, a *Time-Dependent* solution operation will be used.

3.2.1 Calculating the Electric Field

Equation 2.11 needs a physic that can compute the electric field, set the boundaries for the DC-Voltage and others. *Electrostatics* has Poisson's equation built in and will therefore be chosen as the first physics. To implement the charge conservation equations for electric equations (according to Gauss' law), the *Charge Conservation* sub-node is used for all domains. It accounts for the left-hand side of equation Poisson's equation 2.11. It also handles the permittivity, which has been set in the previous chapter. The *Initial values* sets an initial electric potential to the model, which in this case is set to x. This is to prevent division by zero when starting the simulation, since it gives a value instead of zero. Due to charge carriers being an important part of the behaviour of the model, the *Space Charge* sub-node adds a start value for the space charge density to the different intervals (depending on the amount of negative and positive charges). To set a value for the electric potential at the different electrodes, the *Electric potential* sub-node is set to the anode while the *Ground* sub-node is set to the cathode boundary. The *Concentration* setting in the *Discretization* of the *Electrostatics* can in most cases be set to *Linear* with good results. In this case however, it is set to *Quadratic* to compensate for calculation problems that occurred during the build-up of the model.

3.2.2 Transport of charges in the material

The transport of charges in different materials is dependent on the equations 2.9, which therefore needs to be implemented in the model. It can be done in different ways, the most efficient way is to use the *Transport of Diluted Species*. This physics has all the equations needed for the velocity in equation 2.7, the diffusion in equation 2.8 while also having the nodes for the injection equation 2.13. Using the *Transport of Diluted Species* physics, one is used for the positive charges and another one for the negative charges. The main physics node is defined as having *Convection* active while also having the *Conservative form*, i.e. the convective flux of the charge carriers is under the divergent symbol to make it the same as in 2.9. The *Convection and Diffusion* sub-node is used to define the velocity of the charge carriers, using the minus sign for the negative charge carriers, and defining the diffusion. The *No Flux* sub-node main use is to make sure that there is no flow through the electrodes when needed. This is done by including the *Convection* in the point where the specific charge carrier should not pass through. *No Flux* and *Convection*

is used to simulate the behavior of charge carriers at the interface between the epoxy and the pressboard, since the epoxy is there to stop the ions inside of the pressboard to leave it. The initial concentration of charge carriers is specified using the *Initial Values* sub-node, while the reaction rate is defined in the *Reactions* sub-node. Both of these are defined on the whole domain. Finally the concentrations of ions at the boundaries between the electrode and the materials is defined by the sub-node *Concentrations*, where if there is no injection it is defined as zero while with injection it is defined depending on the polarity of the electrode. As for the *Electrostatics*, the *Concentration* setting of the *Discretization* is defined as *Quadratic* to compensate for computational problems during the build-up of the model.

3.2.3 Mesh used in the simulation

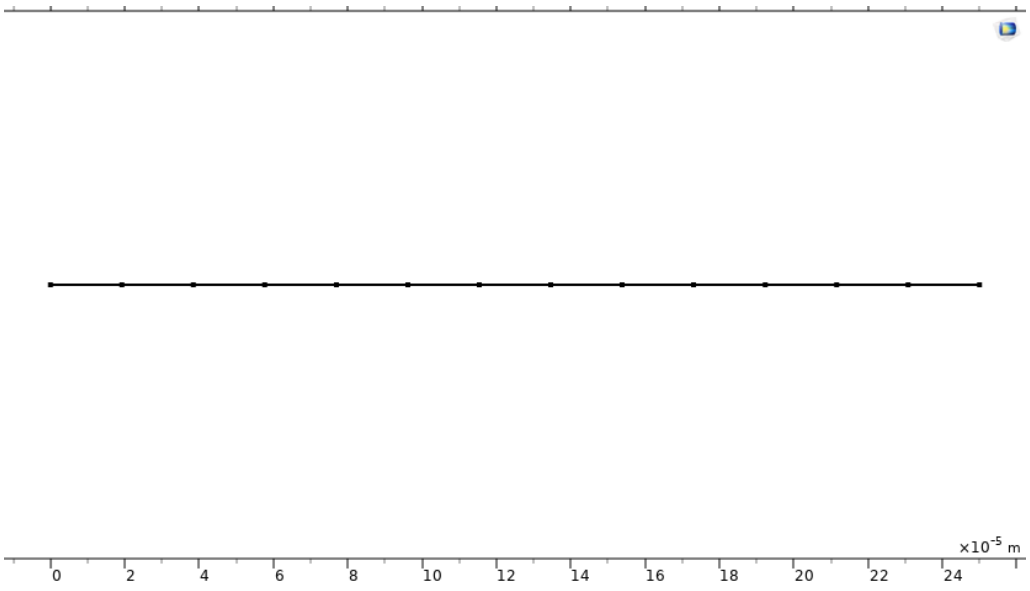

Figure 3.2: Mesh of the Pressboard 1D model

The mesh is the part of the model from which points the results are being calculated. The mesh therefore impacts the calculations significantly, which also makes the resolution of the mesh important depending on the resolution that is needed for the simulations. The mesh in this model is defined to simulate the results of the PEA measurements that have been made in [4] and [5]. From [5], it is defined that the spatial resolution of the PEA measurements are $20\mu m$, which is then implemented into the mesh in this simulation. This should give a similar spread out effect on the space charge density, which when given the correct inputs should give a similar result as in [4].

3.2.4 Stabilization of the solution

For stabilization, only the *Inconsistent stabilization* part of stabilization is used. This is used to combat oscillations that can occur which can prevent the whole solution from converging. This is best done by using the *Isotropic diffusion* stabilization, whose value will depend on the amount of oscillations that occur. The values used in this thesis vary between 0.1 to 0.5, which is within reasonable limits.

3.3 Properties affecting the ion-drift

The oil-impregnated pressboard is constructed by impregnating the pressboard with oil during high temperatures. The porosity of the pressboard is filled by the oil, which affects the properties of the pressboard while affected by an electric field. This is due to the different properties of the materials, where oil has a low dielectric constant while the pressboard having a significantly higher one, or that they have different conductivities [11]. The conductivity of the pressboard have been seen to range between $1 * 10^{-12} S/m$ to $1 * 10^{-16} S/m$ [12] depending on the density of the pressboard and the conductivity of the transformer oil. The dielectric constant is also dependent on the pressboard and the oil, ranging between 3.4 to 4.5 [9]. All of these values are dependent on the temperature and moisture content of the pressboard, which changes over time with the aging of the pressboard and will affect the values in different ways [13]. That the pressboard has such high dielectric constant and low conductivity defines it as an dielectric. The oil-impregnated pressboard simulated in this model has properties that have been chosen to be well within the limits of the values that the permittivity, conductivity and the mobility of positive and negative ions. The chosen values have been taken from [4] and [14]. The chosen values are defined in table 3.1.

Table 3.1: Properties of the oil-impregnated pressboard

Properties	**Values**
Relative Permittivity	3.5 [14]
Conductivity	$1.4 * 10^{-14}\ S/m$ [4]
μ_p	$1 * 10^{-14} m^2/Vs$ [14]
μ_n	$1 * 10^{-14} m^2/Vs$ [14]

The epoxy that is not in this model but instead simulated in other ways have properties according to [4], which gives it a resistivity that is much higher than for the oil-impregnated pressboard. These properties define it, as the pressboard also does, as an dielectric. From

Table 3.2: Properties of the epoxy

Properties	**Values**
Relative Permittivity	3.85 [4]
Conductivity	$1.7 * 10^{-17}\ S/m$ [4]

the values of the pressboard in 3.1 and 3.2, it can be seen that while there is a similar value in permittivity. This will lead to an electric field distribution very similar all over the model at the start. The difference in conductivity will stop the ions from moving into the epoxy, creating the insulating effect that is wanted. The conductivity also affects the electric field over the different materials. Since in 2.3 there is a simplification to the average field over the whole model, this will at first be not considered a factor if it is not needed. If needed, additional simulations will be needed to compensate for the reduction in electric field over the pressboard while the mobility will still be dependent on the average electric field.

3.3.1 Field enhanced dissociation inside the pressboard

In standard pressboards, the equation 2.3 is not valid due to the pressboard being a solid object. With the impregnation of oil, this may no longer be true and some dissociation may be taking place. This dissociation is in this case assumed to only occur in the oil, with the amount of dissociation taking place will, as in equation 2.3, depend on the electric field. It will also be dependent on the recombination and blocking that the pressboard will affect on the ions. Therefore the effect will be to a lesser degree to that of transformer oil. The permittivity of an oil-impregnated pressboard is dependent on the amount of oil that has been absorbed, due to the lower dielectric constant of oil. From this, it is possible to calculate the amount of oil that has been absorbed. The value chosen for this thesis to test is 35.5%, which is a smaller value than the actual one (38.8 % for a dielectric constant of 3.5) [15]. This is lower so to compensate for the other phenomena inside the pressboard. It could also be constant and not dependent on the electric field, both possibilities will be investigated.

3.3.2 Injection from the Epoxy

The injection from one material into another is dependent on the Schottky effect in equation 2.13, which is dependent on the conductivity of the different materials. The conductivity of the epoxy is 1000 times higher than the pressboard, reducing the injection significantly. It is however dependent on the electric field and may therefore be a factor depending on how high the electric field is. Therefore the electric field will be important to verify if there is an impact on the injection into the pressboard. The injection will be the same from both the anode and the cathode side to see if there is any difference in results with high injection at both sides. The epoxy will also affect the electric field, since its much higher resistivity than the pressboard. Its impact will be discussed in section 3.3.5.

3.3.3 Apparent injection from the double layer

The injection from the electrical double layer described in chapter 2.2.1 and equation 2.13 from [7] is different from the injection from the epoxy. When a ion pair is dissociated in the electrical double layer in the oil impregnated pressboard next to the interface between the oil impregnated pressboard and the epoxy, one polarity will be injected into the pressboard while the other polarity is trapped at the interface. If the resistivity of the epoxy is high, the ions trapped on the surface will stay there since they can not be transfered into the epoxy or neutralized by it. This is more complex to implement than the injection from the epoxy and was not included due to time constraints.

3.3.4 Field dependent mobility of ions

The mobility of ions inside an oil-impregnated pressboard has since the interest to study the effect ions have on the insulation properties of materials been a question on how it behaves. At low fields, values stabilize depending on the density of the oil and the density of the pressboard according to [5]. At higher fields, it is not as clear as to how the mobility is dependable on the electric field, the type of ion or the way the ion was created. What is known is that the mobility is decreased in comparison to transformer oil due to the structure of the pressboard. Using the apparent mobility results of earlier

work [4], the feasibility of all ions in the pressboard being dependent on the electric field will be evaluated. It should be noted that these values are defined as the field dependence of injected ions in [4], which in this case will instead be defined for all ions. A thermal equilibrium mobility with differences in value between positive and negative ions will also be investigated. In reality, this does not add any difference in mobility between positive and negative ions, unless the equilibrium mobility is used for all mobility dependent factors. It instead reduces the equilibrium concentration of charges in equation 2.6. A three to one difference in equilibrium mobility can be replaced with doubling the mobility of both positive and negative ions and give the same results. Only differences in mobilities not affecting the equilibrium will affect the mobility.
To implement this, it would be most reasonable to assume that the value S in equation 2.29 is equal to zero, i.e. the sum of trapping, detrapping, recombination and ionization is zero, and using the field dependent mobility in section 2.3. This aspect was realized late in the work and there was not time to implement it, therefore in this work the value of S is not zero.

3.3.5 The electric field during the simulations

As mentioned before, the epoxy will impact the electric field distribution over the pressboard due to its much higher resistivity. Since the electric field in reality spreads out over the model depending on the resistivity and the permittivity of the materials, this should impact the results. The permittivity is close enough between the two materials, so it should not affect the results in a significant way. In the laboratory results [4], it is not specified how the electric field is distributed. It is focused instead on the field dependency of the mobility, which uses the average electric field as stated before. Due to this, the simulations will start with the average electric field being implemented over the pressboard. If this does not achieve the desired results, the compensation for the epoxy will be made. This will decrease the electric field altogether and make the mobility's dependency on the electric field the only factor that will impact the simulations. The potential will therefore start at $6182.8V$, since this is the potential that would give the same electric field over only the pressboard as $23000V$ would give over the whole sample (including the two epoxy).
The second part of the simulations will instead feature a voltage of $41V/mm$ to simulate the effect of the epoxy in the sample, since it reduces the electric field drastically. This will affect the results and affect how the calculations and the field dependent mobility is affected.
These two different parts can be defined as two different cases depending on *Poisson´s* and *Lagrange* equations. For $t = 0$, there is no space charge density and the voltage is distributed capacitively due to the permittivity of the materials. Due to the similar dielectric constant, the voltage is evenly distributed. This can be defined as what happens as the high electric field case. If $t \to \infty$, the electric field instead distributes instead due to Ohm's law due to the difference in conductivity of the different materials. This can be explained for the lower field cases in the following simulations. In an ideal simulation model, the transient voltage drop over the oil-impregnated pressboard should be calculated for each time step and used for each time step. This will lead to the distribution at the start being fully capacitive and then slowly approaching a resistive field distribution with the increase in time. This would implement the charge dynamics in a proper way, treating it with a proper voltage drop over the pressboard at each time step. This was not done in this work due to time constraints, so which of the two different cases that will most closely resemble the PEA-results will be seen in the next chapter.

4

Results

This chapter is about the simulations that were made to try to replicate the earlier laboratory results that can be seen in [4].
Simulation with different parameters and conditions were made. The simulations were performed for 1800 seconds (or half an hour) to have similar conditions as the PEA measurements in [4]. Simulations were made for field dependent, non-field dependent different mobility situations and combinations of these factors to recreate earlier results. All simulations has a equilibrium mobility, which either is altered to see the results or adds a mobility for the higher electric fields. If there is not a figure included, it is not of interest, has a low variation or has a similar result from earlier. In case of negative and positive ions concentrations, if one of the figures are not included, it is due to both having the same results at a different electrode.
The electric field has been defined so that it is the average electric field over the oil impregnated pressboard sample. This is changed in later simulations, where it will be the average electric field over the oil impregnated pressboard that is dependent on the voltage drop over the epoxy that is used as a blocking material.

4.1 The desired results to achieve

The goal of this report was to try to replicate the PEA measurements of [4] using a Ion Drift model in COMSOL. The ways to implement the PEA method was discussed in section 2.3 and has been used in the following results. The results that the laboratory measurements produced by the PEA measurements in [4] has been replicated and can be seen in figure 4.1.

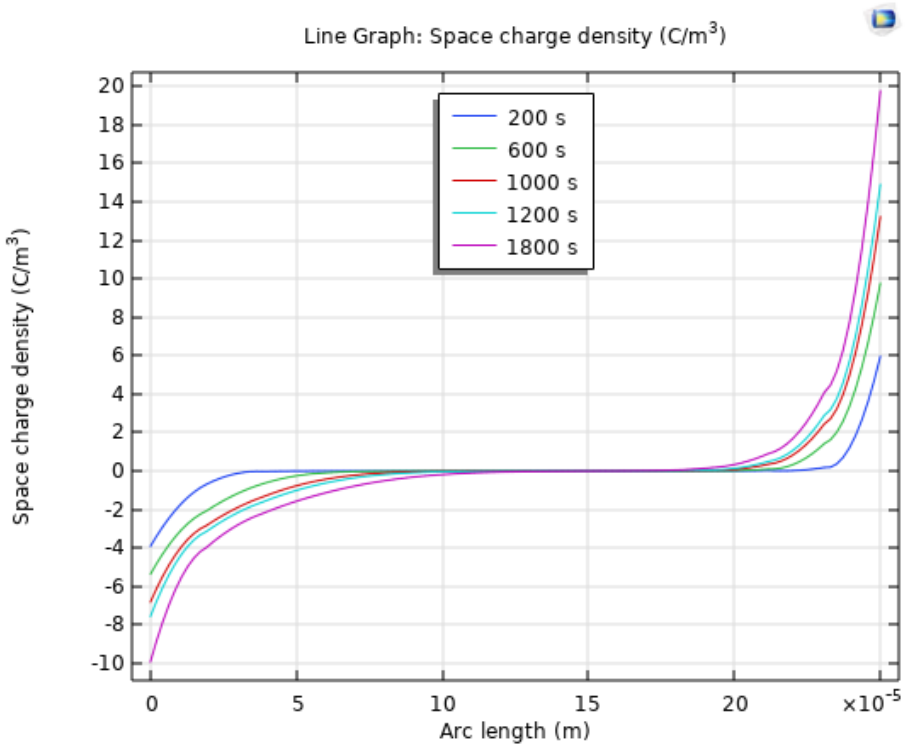

Figure 4.1: Laboratory PEA-results, reproduced from [4]

From this figure, it can be seen that the space charge density at the interfaces increases by time, with higher density at the negative cathode than at the positive anode. The space charge density is also more spread out near the anode when the time is increasing, showing that the ions are moving but that they are not moving fast. The measurements will be mirrored in this report, with the anode to the left in the simulations instead of right in the measurements. Note that it is only the part in [4] that is the oil impregnated pressboard that is simulated here, while the rest of the test object is simplified. It can also be seen that the values for the space charge density should land around $20\ C/m^3$ at the cathode and $10\ C/m^3$ for the anode.

4.2 No field dependency

To try to simulate and recreate the results in figure 4.1, it was considered beneficial to have a reference point where nothing is dependent on the electric field. While nearly all variables are in some way dependent on the electric field, a field-independent model where neither the ionization, the injection or the mobility is dependent on the field can show what behavior the model has without the effect of the electric field and give a reference point if it looks the least similar to the desired results. Therefore a simulation was made where no parameters or variables are specifically dependent on the electric field. First a simulation where there is no difference in the equilibrium mobility between positive and negative ions to see what shape and form the space charge densities takes with a neutral simulation. The results can be seen in figure 4.2.

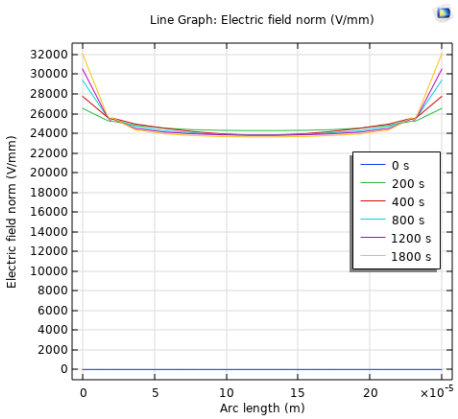

(a) Electric Field

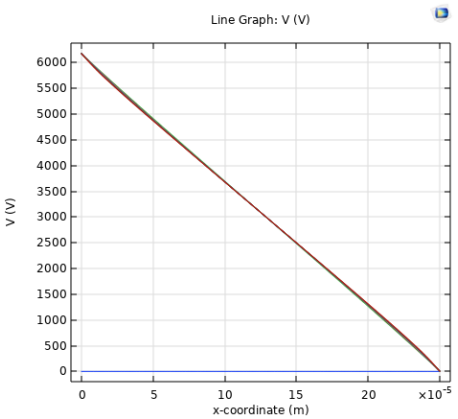

(b) Electric Potential

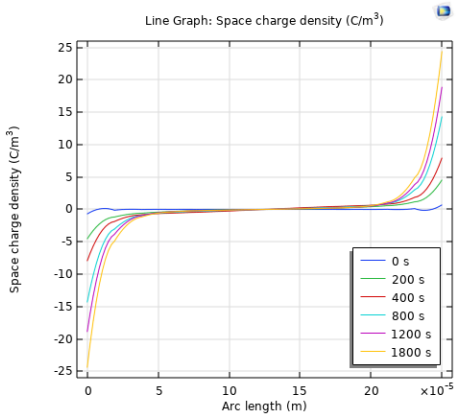

(c) Space Charge Density

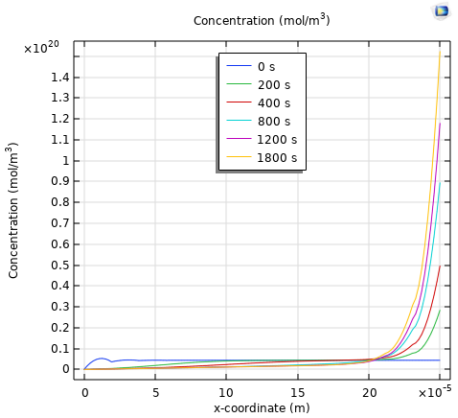

(d) Concentration of positive ions

Figure 4.2: Results of simulation with no field dependency

It can be seen that there is no difference in space charge density between the anode and the cathode, suggesting that there needs to be a mobility difference to realize the desired results. The electric field becomes stronger at the ends due to the higher concentration of ions as expected, while else being spread out evenly over the interval. The potential decreases nearly linearly over the whole interval, suggesting that the differences in space charge density does not impact the voltage division in any significant form.. The values of the space charge densities at the anode and the cathode are in the same magnitude as the PEA measurements in [4], indicating that it is possible that the ionization may not be field dependent. The positive ion concentration and the negative ion concentration achieves the same values (though only the positive concentration is shown), which is expected due to the same values in mobility.

4.2.1 Different mobilities for positive and negative ions

Since the calculated mobilities in the earlier work such as [5] indicates a difference in mobility between positive ions and negative ions, two simulations with either a 2 to 1 difference in mobility or a 3 to 1 difference in mobility is made to see the impact the change in the mobility has on the results. According to the report, it should be the negative ions that move faster than the positive ions. From the results in figure 4.2, it is

expected that there should be some differences in space charge density between the anode and the cathode. It should also affect the equilibrium concentration in equation 2.6, due to the change in mobility. The results of the simulations with no difference and the results of the 3 to 1 difference can be seen in figure 4.3.

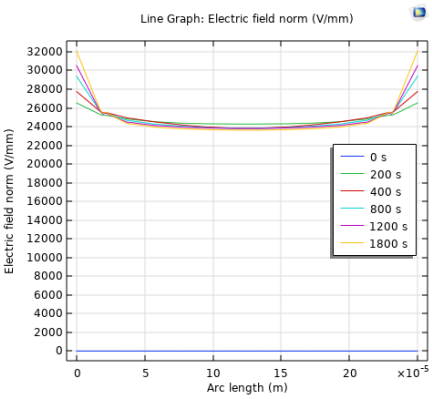

(a) Electric Field - No Diff

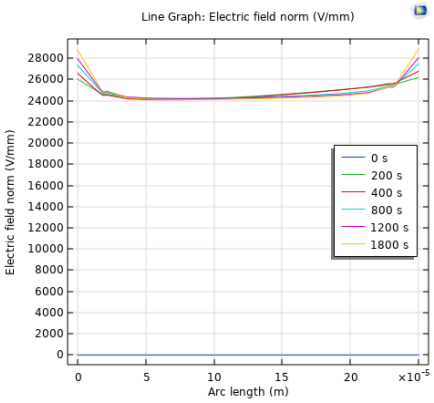

(b) Electric Field - 3 to 1

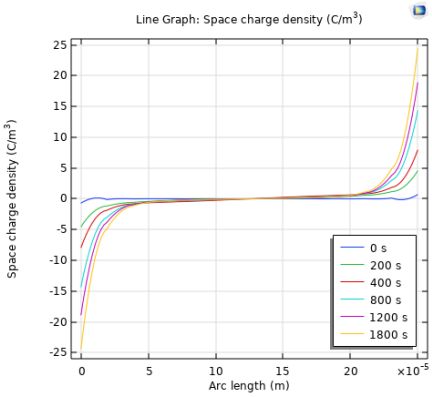

(c) Space Charge Density - No Diff

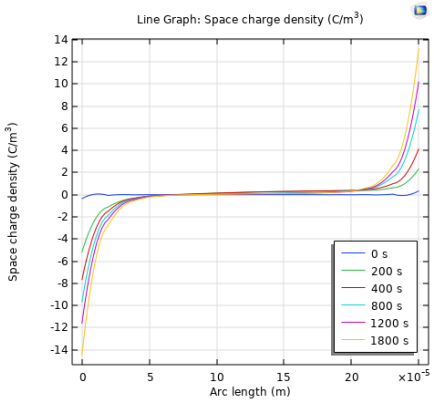

(d) Space Charge Density - 3 to 1

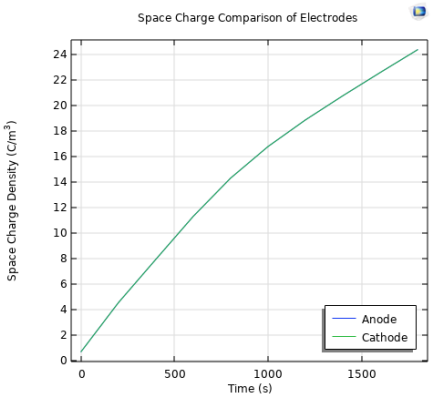

(e) SCD at electrodes over time - No Diff

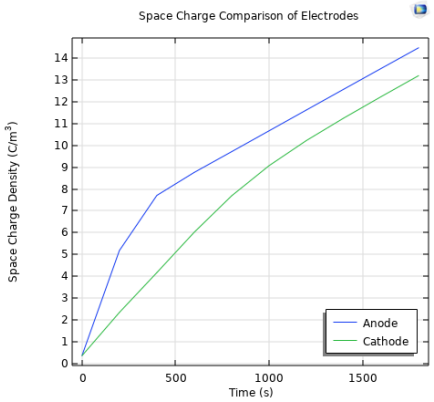

(f) SCD at electrodes over time - 3 to 1

Figure 4.3: Results of simulation with no field dependency and different mobilities

From the simulations, it can be seen that the change in equilibrium mobility changes the spread of the space charge density and the electric field. The difference between the space charge density over time between the anode and the cathode rises the first 400 second, which afterwards levels out after a linear state has been achieved and seems to go towards the same value if the simulation would have continued. The higher value in space charge density is at the anode, which is opposite from the results of the PEA measurements in [4], while the magnitudes are smaller than the results achieved there. The larger difference in mobility also reduces the top values of the space charge density.

4.3 Single field dependent factor

The three factors that possible to be field dependent was simulated. Simulating each of the three factors that may affect the results of the simulations are highly valuable and will rule out factors that does not affect the results. First all factors were simulated without any difference in the mobility.
Ionization is field dependent in transformer oil, however it has been defined not to be field dependent in oil-impregnated pressboard before. Therefore it is especially interesting to see if there is any effect of it. The results are shown in figure 4.4

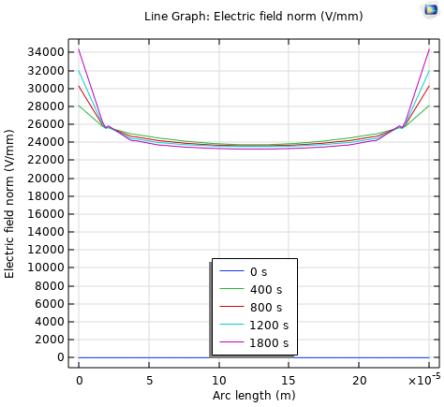

(a) Electric Field

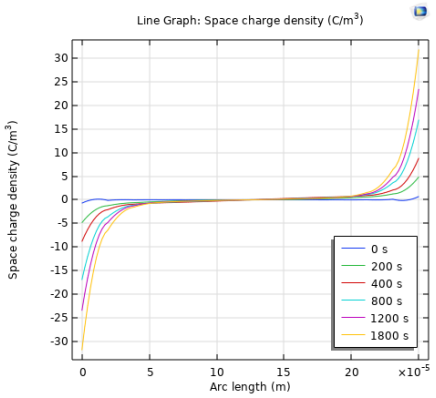

(b) Space Charge Density

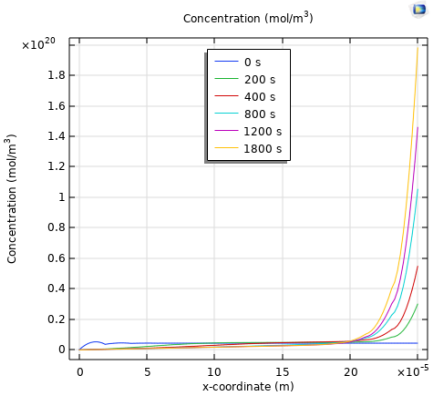

(c) Concentration of positive ions

Figure 4.4: Results of simulation with ionization being field dependent

The results can be seen are similar to the results for the non-field dependent simulations in 4.2, with linear loss in potential and even spread out of the electric field. The electric field have higher values at the boundaries, which can be explained by the higher values in space charge density, which in turn is dependent on the higher value of concentration of ions. The values of the space charge density are about 40% higher with the field dependent ionization than with no field dependency. This values are a bit high, which may decrease when simulating different equilibrium mobilities later.

Since the epoxy is encapsuling the pressboard, it is expected that no injection should be impacting the pressboard. It is still important to simulate, which results can be seen in figure 4.5

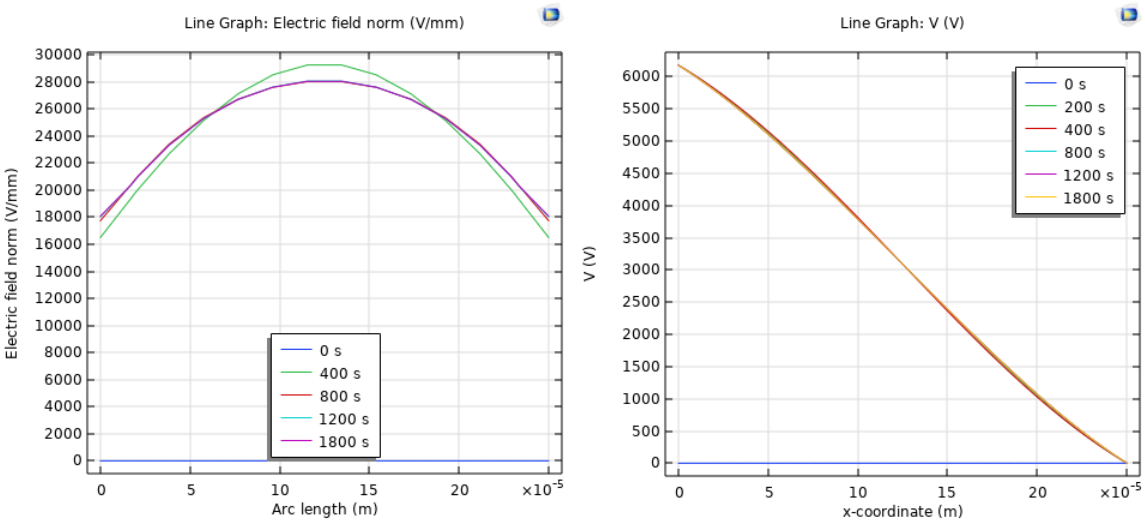

(a) Electric Field **(b)** Electric Potential

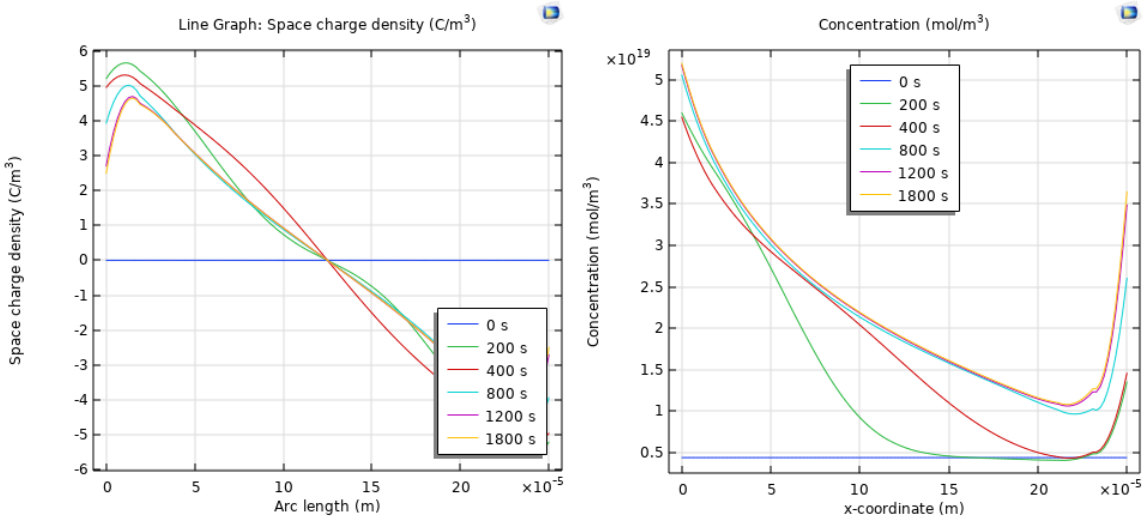

(c) Space Charge Density **(d)** Concentration of positive ions

Figure 4.5: Results of simulation with injection being field dependent

The results from the simulations of the injection being field dependent are significantly

different from the earlier simulations and are not similar to the earlier results in figure 4.1 that this model is trying to replicate. The positive ions are high close to the anode instead of the cathode, indicating homocharges, while the opposite is true for the negative ions. The electric field is higher in the middle of the interval instead of close to the electrodes. The electric potential also have a more curved form, indicating the effect of the injection. For the positive ion concentration, the higher values are at the injecting anode, while a small increase can be seen towards the cathode due to the attraction of opposites

It is however clear that this does not replicate the desired results, with too high space charge densities and the higher magnitude of positive and negative ions being at the electrode with the same polarity.

Mobility field dependency has been proposed and estimated from measurements in [5] and [4], which indicates a difference in mobility from the beginning. First simulations were performed were the mobility was defined to be dependent on the electric field strength. The equilibrium mobilities are defined as the start value and being the same for positive and negative ions, These equilibrium mobilities are not affected by the electric field. Results can be seen in figure 4.6 and in figure 4.7

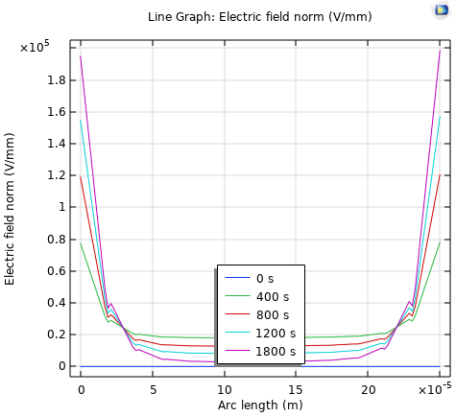

(a) Electric Field

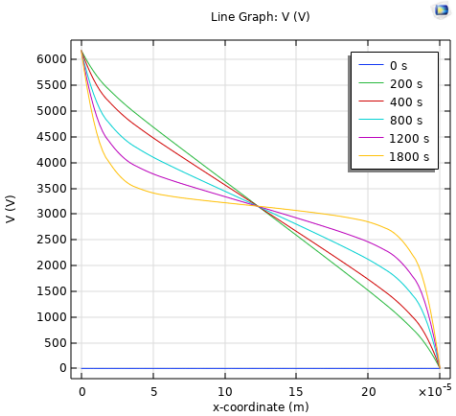

(b) Electric Potential

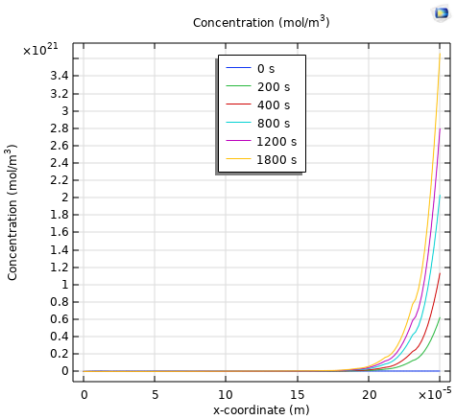

(c) Concentration of positive ions

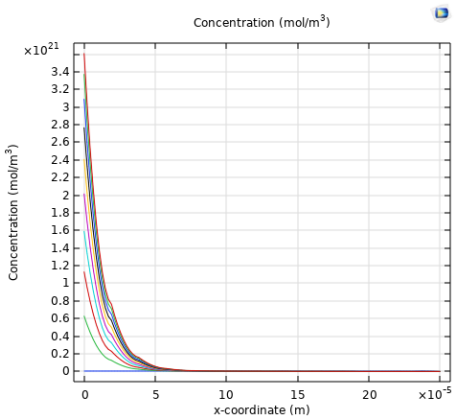

(d) Concentration of negative ions

Figure 4.6: Results of simulation with mobility being field dependent according to the analysis of PEA measurements in [4], part 1

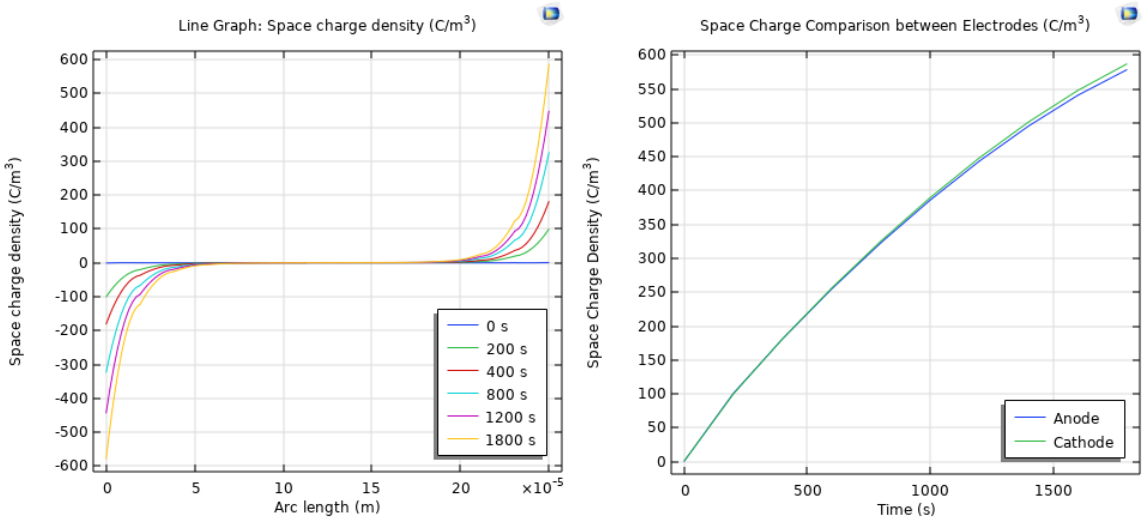

(a) Space Charge Density

(b) Space Charge Density at electrodes over time

Figure 4.7: Results of simulation with mobility being field dependent according to the analysis of PEA measurements in [4], part 2

It can be seen that the difference in space charge density between the anode and the cathode exists. While small at the beginning, it becomes more visible the longer the simulation runs. This indicates that a steady state has not been reached, which is different from all previous simulation. It can also be seen that the electric field is significantly spread out, with high peaks close to the boundaries. This can also be seen in the potential graph 4.6b, where the potential drop is high closer to the boundaries while small in comparison in the bulk of the pressboard. The values of the space charge density is many times higher than the previous values and also the higher value is at the wrong electrode, making these results too impactful to be reasonable. These high space charges may come from double counting in the model, this due to the value of S in equation 2.29, as discussed in section 3.3.4, is not zero and therefore will contribute to the space charge density. It does however have a shape similar to the desired results, so it will still be simulated in later simulations.

4.3.1 Polarity dependent mobility

From [5], there seems to be evidence that there are difference mobilities for the positive and negative ions at low fields, which will impact the equilibrium concentration of ions. Therefore this impact needs to be simulated to see if it affects the results, using a negative mobility being either twice of thrice the size of the positive ions. Starting with the ionization being field dependent and with different start mobilities, the results can be seen below in figure 4.8.

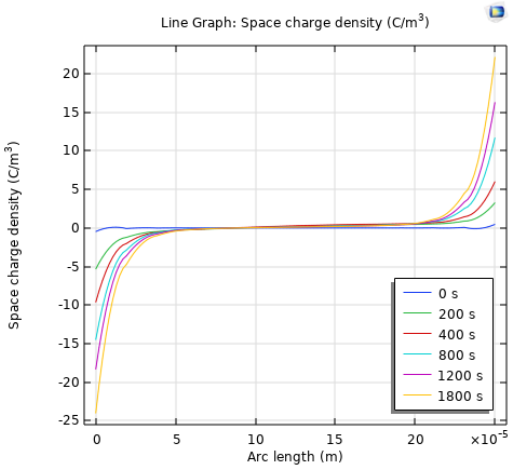

(a) Space Charge Density - 2 to 1

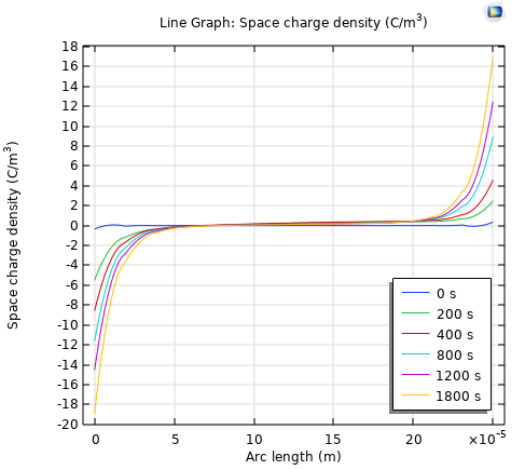

(b) Space Charge Density - 3 to 1

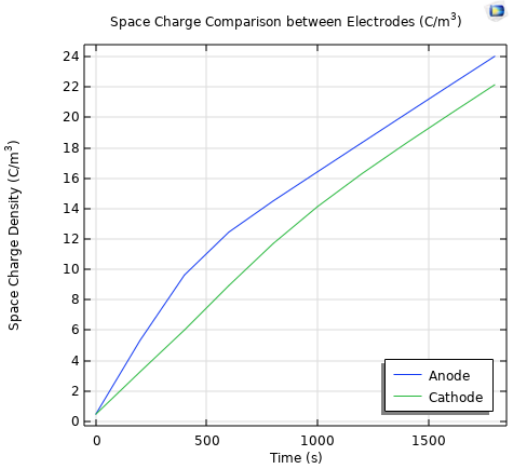

(c) Space Charge Density at electrodes over time - 2 to 1

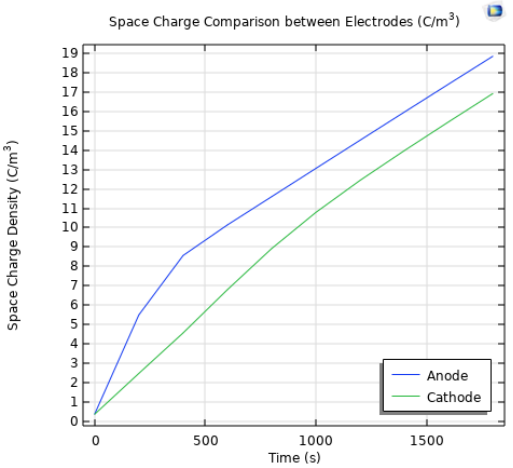

(d) Space Charge Density at electrodes over time - 3 to 1

Figure 4.8: Results of simulation with ionization being field dependent and different mobilities

Comparing figure 4.8 with the earlier results in figure 4.4, there is a clear difference in space charge density. In figure 4.8, the difference between having a difference in mobility of two or three times can be seen in the space charge density at the electrodes over time. This also increases the difference between the space charge densities at the different electrodes, which makes these results more similar to the PEA-measurements. The difference between the simulated and the laboratory results are still significant, since the difference in value of the space charge density at the anode and the cathode is still much smaller and also opposite in which has the higher value. The higher difference in mobility have a small impact before 600 seconds, but comes to a steady state as the lower mobility difference.

The injection without any difference in equilibrium mobility did not give results in any vicinity of the desired ones, however it is still important to simulate to be able to discard it as a possibility. These new similations are seen in figure 4.9.

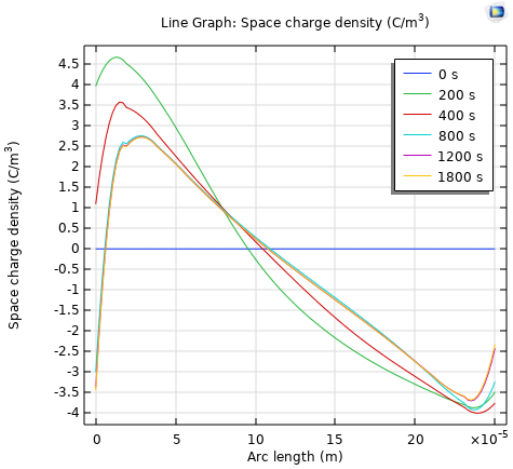

(a) Space Charge Density - 2 to 1

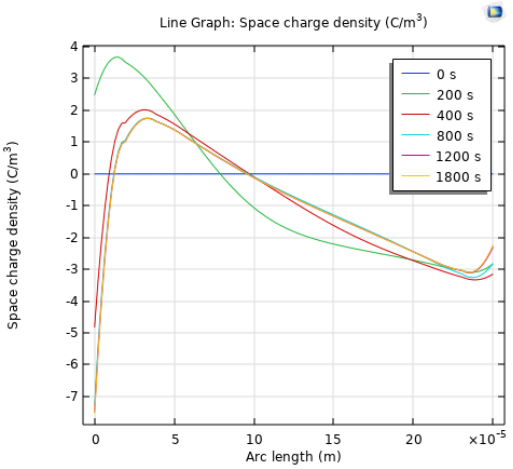

(b) Space Charge Density - 3 to 1

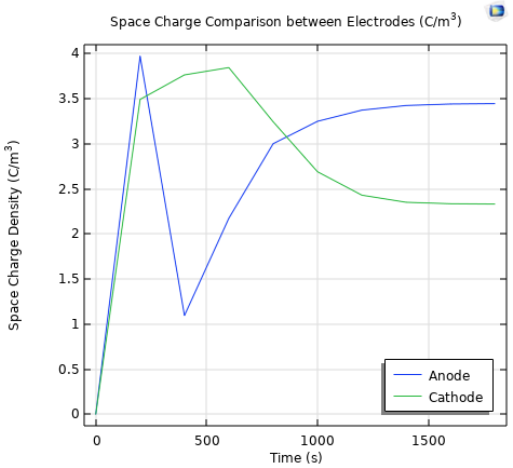

(c) Space Charge Density at electrodes over time - 2 to 1

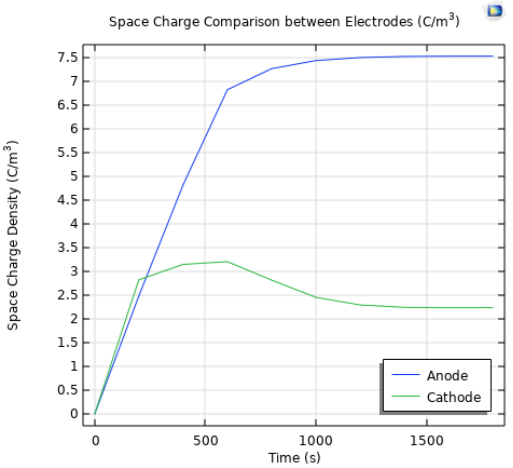

(d) Space Charge Density at electrodes over time - 3 to 1

Figure 4.9: Results of simulation with injection being field dependent and different mobilities

That there is a difference between injection with no difference in mobility and with difference in mobility is clear, while also the difference in how much mobility difference there is can be clearly seen. It still does not look like the measurements that this model should achieve in the end. The only change the difference in mobility did was to reduce the magnitude of the space charge density and shift the space charge density more towards the cathode. The space charge densities over time for the 2 to 1 polarity dependent mobility is strange and may be due to small sample size.

The field dependent mobility was then simulated with difference in equilibrium mobility. This does not impact the field dependency, only the start value of the concentration. It does not decrease that significant for it to come close to the desired values and are therefore not of interest.

The simulations above indicates that not all factors may impact or help reach the de-

sired results, which indicates that either combined factors or other parameters may be impacting the results of the laboratory measurements. The ionization field dependency, the mobility field dependency and the non-dependent models have given the closest results so far, while the injection does not seem to impact the results. The latter is a positive trend, since the epoxy is supposed to eliminate the effect of the field dependent injection. More simulations is needed since the previous simulation does not show the results that is desired. Next up is to test the combinations of several or all possible field dependent factors.

4.4 Influence of several field dependent properties

SFD The results from section 4.3 do not align with the results that this report is trying to replicate. It therefore seems to be either something wrong in the values themselves or that several factors may be combining to create the results seen in the laboratory. The ionization and injection have been defined as field dependent for the transformer oil [1], which is one part of the oil-impregnated pressboard. Earlier results indicate that the injection should not impact, while the ionization field dependency is debatable. Therefore, combinations of factors that may be field dependent are combined and simulated in figure 4.10. Note that for the same equilibrium mobility, the mobility and ionization field dependent model did not finish the simulation due to the values increasing too high. That combination can therefore be disregarded if there is equal mobility in equilibrium.

The results of ionization-injection, mobility-injection and all three factors being field dependent can be seen in figure 4.10 and figure 4.11.

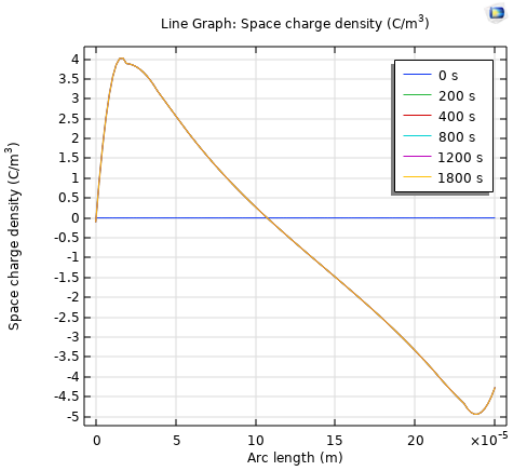

(a) All field dependent - Space Charge Density

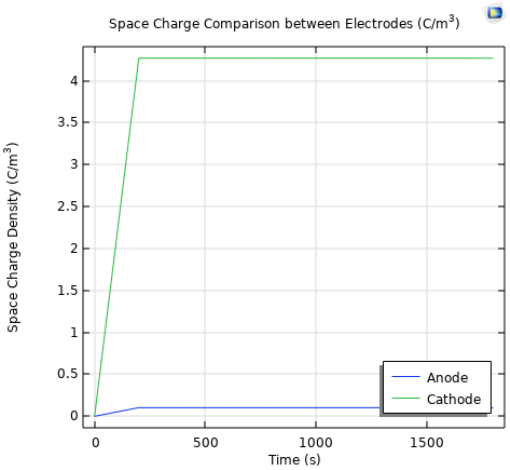

(b) All field dependent - Space Charge Density over time

Figure 4.10: Results of simulation with several factors being field dependent with same equilibrium mobilities - Part 1

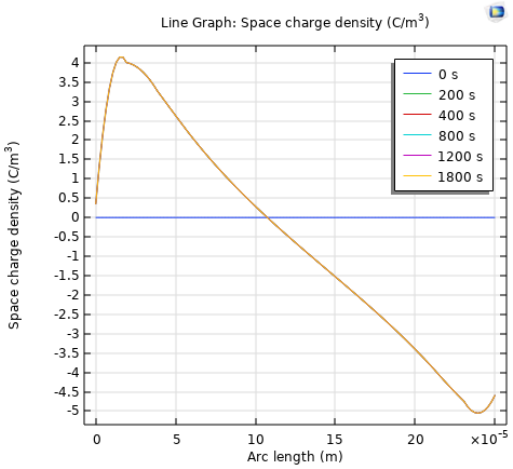

(a) Injection & Mobility Field Dependent - Space Charge Density

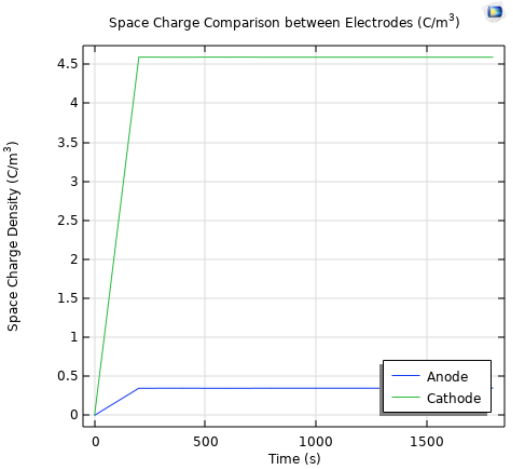

(b) Injection & Mobility Field Dependent - Space Charge Density over time

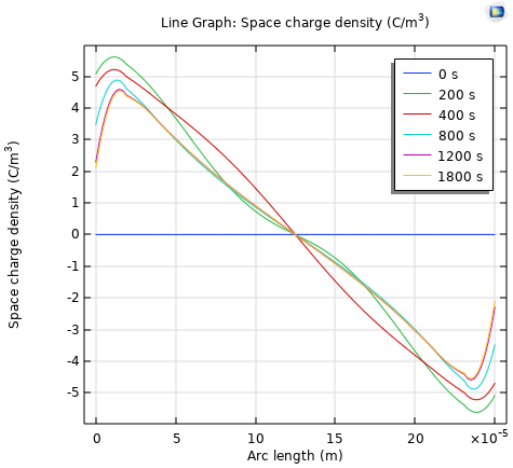

(c) Ionization & Injection Field Dependency - Space Charge Density

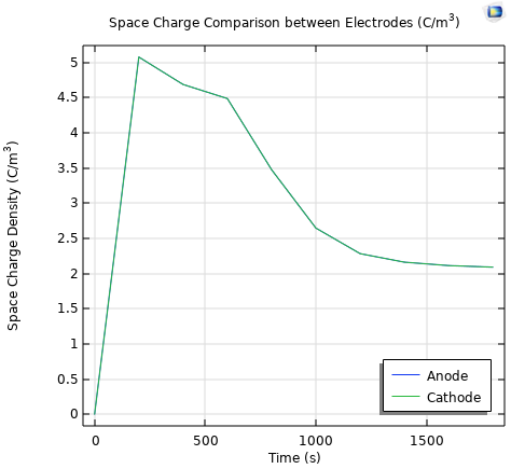

(d) Ionization & Injection Field Dependency - Space Charge Density over time

Figure 4.11: Results of simulation with several factors being field dependent with same equilibrium mobilities - Part 2

Since the results desired have a higher concentration of positive ions near the cathode while the negative ion concentration is higher at the anode, any results that significantly contradicts these results are dismissable. None of the results using different combinations of factors together gives an result close to the results given by the earlier PEA-results. Positive and negative ions have a higher concentration near the electrode with the same polarity. There is one more combination that is of interest, the ionization and mobility field dependency. For equilibrium mobility values being the same, the space charge densities goes towards infinity and are therefore not valid. A difference in 2 to 1 in equilibrium mobility gives the results in figure 4.12.

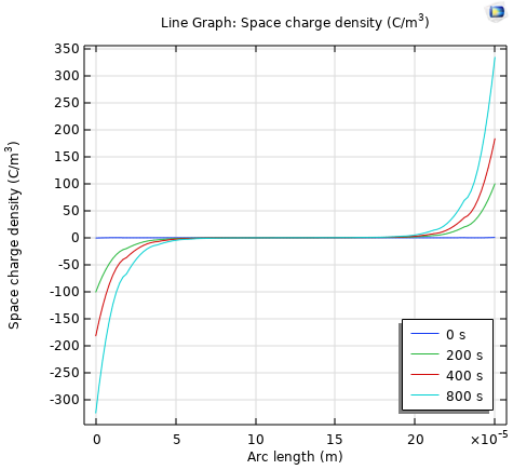

(a) Ionization & mobility Field Dependent - Space Charge Density

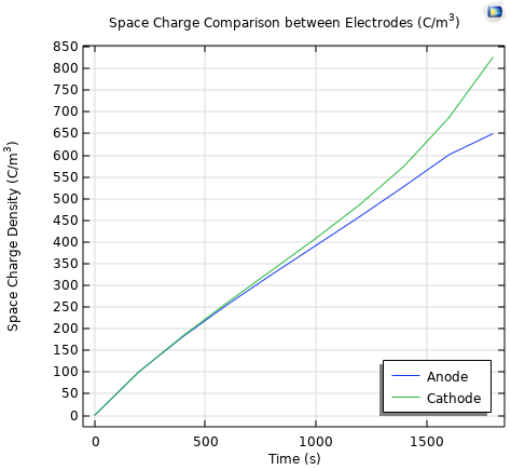

(b) Ionization & mobility Field Dependent - Space Charge Density over time

Figure 4.12: Results of simulation with ionization and mobility being field dependent with a 2 to 1 relation in mobility

The peak values of the space charge densities at the different electrodes are much higher than in the PEA-results, while it also has started to deviate from the linear behavior and instead starts to increase the difference between the anode and the cathode. This may explain the failed simulation with similar equilibrium mobility, since it could have led to the value going towards infinity. This behavior is not realistic and therefore can be dismissed. This leads to more investigation needed, which will be done in section 4.5.

4.5 Dependency on the electric field & materials

From the results in the previous sections, it can be determined that only the ionization being field dependent or no field dependency at all gives results that are in the same magnitude and shape as the PEA-results in figure 4.1. While the field dependency of the mobility to this point has not given any results close to the desired ones, the visuals of it still is similar to the desired results. It therefore seems to be discrepancies and factors that have not been fully taken into consideration. While the results may be difficult to replicate completely, the theory behind the discrepancies can be explained.

From the results of the PEA-measurements [4] in figure 4.1, it can be seen that the magnitude of the space charge density at the interfaces between the pressboard and the epoxy increases during the whole experiment. It is therefore reasonable to believe that a steady state or linear increase has not been reached until the end of the experiment.

Let's look at the space charge density change at the interfaces for the simulations that have been made before. There is only one for when the equilibrium mobilities are the same, which is the mobility field dependent on figure 4.7b. There is a small increase in difference between the two interfaces, however it seems to increase with time. This is not realistic and is therefore not of interest.Other parts that can be dismissed in the injection field dependency with different equilibrium mobilities, which reaches a steady state

shortly after the simulation has started. The difference in equilibrium mobilities does not have to be there. The only equation the equilibrium mobilities impact is the equilibrium start concentration of ions or equation 2.6. Here the different mobilities are just added together, which leads to the conclusion that it is the start concentration that matters, not the difference in mobility here. With different mobilities, the figures 4.3e and 4.3f relating to no field dependency, figure 4.8c and 4.8d relating to ionization field dependency, and 4.9c and 4.9d referring to mobility field dependency is of interest. In the figures relating to no field dependency and ionization field dependency, it can be seen that a steady state or linear state has been reached around 600 seconds. This alludes to the fact that the electric field over the pressboard is high enough that steady state is reached before the complete simulation is over. With the knowledge that due to the conductivity difference between epoxy and pressboard, it is reasonable to conclude that the electric field over the voltage is too high and needs to be lowered for steady state to be reached later. Therefore the simplification with only calculating on the average electric field needs to be removed and that the actual electric field over the pressboard is the important part. This can be simulated by adding the epoxy as a contact resistance to the model. This will decrease the electric field over the pressboard and give values that are more in line with reality.

From 3.1 and 3.2, it can be seen that the conductivity of the epoxy is over a thousand times smaller. This means that the electric field over the epoxy will be a thousand times stronger than for pressboard at steady state, which will make the electric field over the pressboard in the magnitude of $10V$. While realistic, the field dependency will be non-existent at this value and will not be a factor for ionization. This can be implemented either using a voltage divider to calculate the correct voltage or adding a contact resistance as in section 2.2. Simulating that case, where the potential is instead at $10.25V$ the mobility is kept at the equilibrium values (and same values) for the whole simulation in figure 4.13.

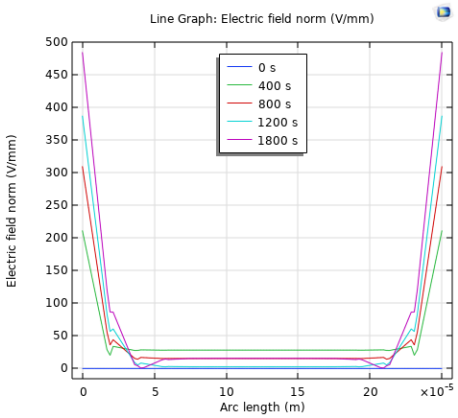

(a) Low field over pressboard - Electric Field

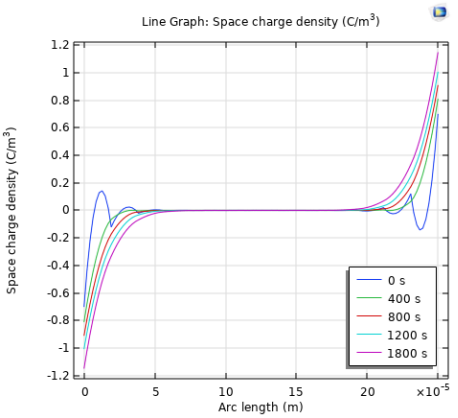

(b) Low field over pressboard - Space Charge Density

Figure 4.13: Results of simulation with very low electric field and high mobility

This gives strange values that are not even remotely close to the values that was found in the measurements in figure 4.1. The space charge density seems to be too small for it to be reasonable. The small overshoots can be explained by the discretization being quadratic as described in section 3.2.

The space charge density is dependent on the equilibrium concentration in equation 2.6, which is dependent on the conductivity of the material and the equilibrium mobility of the ions. The conductivity is not reasonable to change, while the mobility of the ions can be changed down to $1 * 10^{-15} m^2/Vs$. To test the impact and the reasonability of the field dependent mobility, this is also implemented here. The mobility is dependent on the average field, therefore it is taking the average field for the whole sample (including the epoxy). Simulating this with the same mobility after equilibrium and having field dependent mobility, the results can be seen in 4.14. Simulations changing the field dependency of the different ions has also been performed here.

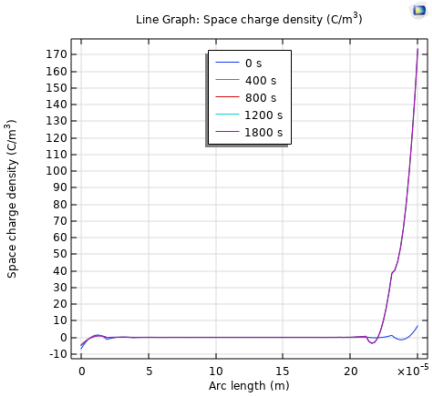

(a) Mobility Field Dependent - Space Charge Density

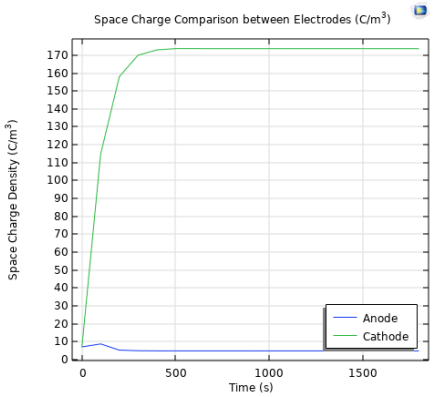

(b) Mobility Field Dependent - Space Charge Density - Opposite

Figure 4.14: Simulation with low electric field, low eq. mobility and field dependent mobility

From the results, it can be seen that the field dependent mobility distorts the results significantly and the behavior is not reasonable. As seen in the space charge density at the electrodes over time in both cases, the lower value electrode drops in space charge density after a short time. These results are not realistic, so a new approach is needed.

With the field dependent mobility dismissed, the goal is to find as close of a result as possible. A result barely distinguishable as different does not seem possible with only changing mobilites, however a result in the correct range was possible with having a significant difference between positive and negative ion mobility after equilibrium. Simulating this with the same mobility after equilibrium and having different mobility for positive to negative (4 to 1) gives the results in figure 4.15.

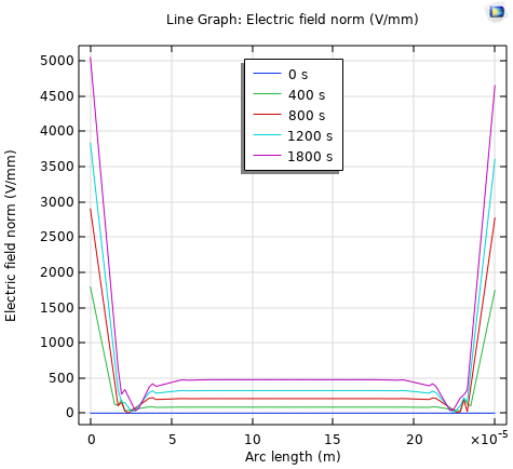

(a) Low eq. mobility - Diff. Mobility - Electric Field

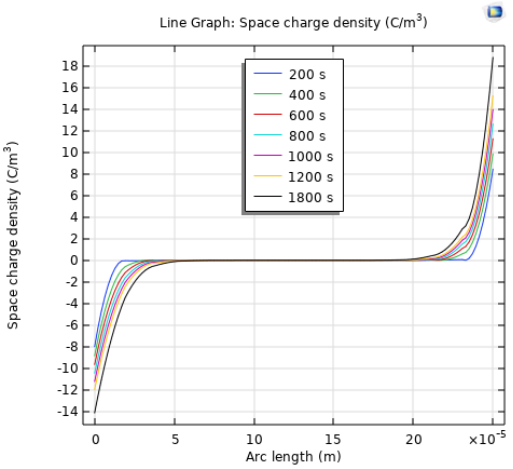

(b) Low eq. mob- - Diff. mobility - Space Charge Density

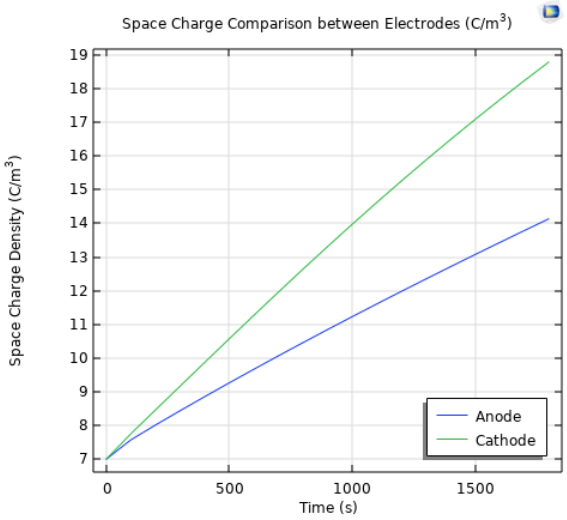

(c) Low eq. mob - Diff mobility - Space Charge Density over time

Figure 4.15: Simulation with low electric field and variable mobilities

The decrease in equilibrium mobility and the difference in mobilities draws the results closer to the values that is desirable. Now the space charge density at the cathode is about 43% larger than at the anode. From now, the equilibrium mobility and the mobility dependency on the electric field is stable and will not be able to contribute more towards the final results with this low voltage. The space charge density in figure 4.15b can then be compared with the results of the PEA-measurements in [4], which can be seen in figure 4.16. Note that the Anode is to the left in the simulated graph.

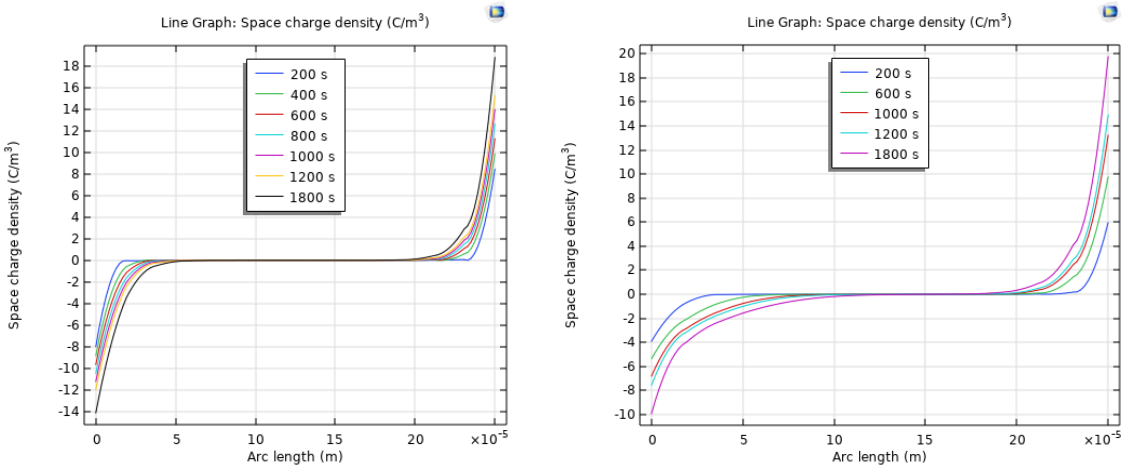

(a) Simulated Space Charge Density **(b)** PEA-measurements recreated from [4]

Figure 4.16: Comparing the simulated values with the PEA-measurements.

The similarities between the simulated values in figure 4.16a and the PEA-measurements in the *OP* region in figure 4.16b can be clearly seen. They are however not so similar that the results can be considered the same. The results are now in the correct electric field, dependent on the conductivity of the materials and dependent on differences in mobility between positive and negative ions.

5
Discussion

From the final simulations in section 4.5, it can be clearly seen that if the simulation results should be anywhere close to the results seen in the PEA-measurements (or figure 4.16, the field dependent mobility must be for the same electric field as over the pressboard, else the results deviates significantly from reality (seen in figure 4.14). This seems to deviate from the results and conclusion found in [4] and questions the field dependency of the mobility. It is possible that the results still are correct, in which case the electric field distribution over the sample needs to be disclosed for a proper examination to be made.

As of the information available from the paper, it must be assumed that the electric field spreads over the epoxy and the pressboard depending on the conductivity and the permittivity, as it would according to *Lagrange* and *Ohm's law* as discussed in 3.3.5. With the over a thousand times lower conductivity of epoxy seen in table 3.2, the field will disproportionately spread over the epoxy and leave a field of around $41V/mm$ over the pressboard. In this field range, the field dependency of mobility and ionization could be ruled out and is therefore not a factor. More research is needed to conclude if there is a field dependency on the mobility, which as of now seems questionable.

This also brings into question the simplification in [4] around the average electric field, since the results do not line up with that statement. This is also dependent on the field distribution during the measurements. The processes inside the bulk of the pressboard can't be defined after the average field and needs to be calculated according to the local field that is time dependent. From the results, it can be seen that a steady state has not been reached by the end of the simulation. This seems to be in line with the PEA-measurements, however it is not certain. This also leads to the results being somewhere in between only the permittivity controlling the electric field distribution (high field case in 3.3.5) and the distribution being dependent on the conductivity (low field case in 3.3.5). Due to the effect of the difference in conductivity, the effect of the permittivity seems to be negligible though the steady state has not been reached.

[4] also seems to make the assumption that the injected charges and the ionized charges inside the pressboard are different in their dependency on the electric field. While there is a higher electric field at the boundary of the epoxy and the electrodes, this is not in line with what has previously been researched.

The simulations made have been made with assumptions around electric field, conductivity, equilibrium mobility of ions and resistivity. This will give results that are not completely accurate, since all the values may not be compatible with each other, however it was accurate enough to see the behavior of the pressboard and find results within the same range as the PEA-measurements. The difference in equilibrium mobility of the different ions can be disregarded, since the effect of a three to one in equilibrium mobility

gives the same result as if both mobilities had been doubled. This can be explained by equation 2.6, where the combined value determines the equilibrium concentration of ions.

The size of the mesh does affect the results, since the mesh in this model has been designed to try to replicate the results of the PEA-measurements as closely as possible. This will lead to distortion of the results, which examples of strange behavior in the figures can be seen in figure 4.15. Here the distribution of the electric field decreases just before it rises to its high points near the boundaries. It can also be seen in the same figures that using *Quadratic* in the concentration discretization for both *Electrostatics* and *Transport of Diluted Species* causes the values to oscillate over their realistic values and go into the opposite space charge. This can be removed by using *Linear* instead, which can cause other calculation problems, which are more problematic to overcome.

The reduction in equilibrium mobility to achieve the final results in figure 4.15 does move the mobilities for both the negative and positive ions closer towards the values that was calculated in [4], while it becomes a significant different when compared to the results in [5]. These reports also define the negative ions to be moving quicker than the positive ions, however this gives faulty results in the simulations if this is implemented. There could be more advanced reasons why this is occuring, the time to find the cause was not available and was therefore skipped.

5.1 Sustainability in Oil-impregnated pressboard

The simplicity of the oil-impregnated pressboard makes it a useful and common insulator for power transformers. Due to the same reason as why it is in higher demands in HVDC systems, it will also need to become a more sustainable insulator for it to not be outmaneuvered or replaced by other insulators when the time comes.

The pressboard itself is made by cellulose, which is a biological material and therefore also renewable. This part of the insulation is therefore from the start more renewable than many parts in the power system. As long as the cellulose is produced from wood that is not increasing deforestation in the world, the process of producing it can be renewable without any significant work needed. The question is more than around recycling, which will be needed for the renewable aspect to become complete for the pressboard.

The transformer oil is made from the same material that fossil fuels are made of, which makes it automatically non-renewable. This is the part of the insulation where the most effort needs to be put to increase the environmentally friendly aspect of the insulation. Using synthetically produced oils that use biological sources is important for the renewable aspect of the oil-impregnated pressboard. Oils such as Ester and Isoparaffin B may be of interest here, since they are both biodegradable [16]. They come with their own drawbacks, which may in the end still be small enough for them to become the dominant sources for the oil in the oil-impregnated pressboard. While much of the used transformer oil today is not renewable, in recent years recycled transformer oil have started to appear [17]. These are refined in an oil refinery and has the same quality as new transformer oil. This at minimum reduces the amount of transformer oil discarded and at best could in the end recycle the majority of the transformer oil that is not renewable.

Due to research and development, some materials may be inserted into the pressboard to increase the electric strength of the pressboard [18]. These materials are an aspect that also needs consideration, since they may be produced by fossil fuels. Therefore efforts towards keeping the use of polymers in transformer insulation to a minimum or only using biodegradable polymers.

If the above aspects of the oil-impregnated pressboard is addressed, the insulation itself will have a significant part in the path towards a renewable and environmentally friendly power system, due to its role within both the AC-power system and the HVDC power system. Its role in the HVDC system is particularly important, since HVDC cables are the only one's used when transferring the produced energy from wind farms out in the water towards the mainland. It is also important when transferring energy over long distances between different countries under water, due to the increased connections between countries around the world.

6
Conclusion

6.1 Main findings from the simulations

This thesis focused on the processes inside the oil-impregnated pressboard and the effect of electric field stress on the material. With earlier work and a modernized COMSOL Multiphysics model, simulations were made to replicate earlier work. From the simulations, it can be seen that the behavior of the PEA measurements is possible to recreate with the Ion Drift Conduction model, as long as the inputs and the parameters are correct. When the pressboard is insulated using epoxy, the effect of the injection is insignificant and therefore not affected in any significant degree when a higher electric field is affecting the pressboard.
The ionization inside the bulk of the pressboard has an effect on the space charge density and is to a point dependable on the electric field. The significance of this effect is debatable, with the difference between an non-field dependent ionization and a field dependent ionization being small in magnitude in comparison with other aspects. When using the contact resistivity-affected potential over the sample, the electric field becomes much lower in value ($41V/mm$) in the sample due to the high conductivity difference between pressboard and epoxy. At this electric field level, the effect of the field dependency of the ionization can be disregarded due to only having an effect at electric field values over $1000V/mm$
The mobility of the ions shows dependency on the electric field, however the magnitude of the dependency can be questioned and needs more research to find a conclusion on. Using the results of the earlier work for the field dependency of the mobility did not achieve the results acquired from the PEA-measurements, most likely due to differences in the electric field over the sample. Using the values the mobility would have in the low electric field that the pressboard is stressed under, results in the vicinity of the measured results are possible to create.
The simplification to the average electric field for the mobility is clearly not useful in any other part of the simulation, due to the incorrect values and the short time it takes for the space charge density to reach a steady state. The results from the PEA measurements are only reproducible before the space charge density has reached its steady state, which is dependent on the level of the potential that is affecting the pressboard.

6.2 Possible future work

From this thesis, several possible roads have not been explored when producing this thesis and the model it is based upon. These could be divided into two groups, one which is focused on the improvement of the model and one that implements more of the detailed structure of the oil and cellulose fibers that makes up the oil impregnated pressboard.

6.2.1 Implementing a time dependent voltage drop over the Pressboard

In section 3.3.5, it was mentioned that this work focused on seeing if the results more resemble a capacitive distribution of the voltage or a more resistive distribution. There was also discussed an ideal simulation model, where the transient voltage drop is calculated and implemented for each time step. This part could be a good future work, since it would implement both the capacitive and resistive distribution of the voltage into the model, bringing the model into a more realistic and more accurate version. This would be a good first step to improve the model.

6.2.2 Implementing apparent injection that charges up the interface

It was mentioned in section 3.3.3 that the apparent injection of the electrical double layer due to Schottky injection was not fully implemented due to time constraints. Implementing this into the model would account for the injection of the electrical double layer that is formed when the oil-impregnated pressboard is affected by an high electric field. It would more accurately implement the injection at high fields and would better accont for the effect of the double layer.

6.2.3 Calculating the field enhanced mobility for the case S=0

As mentioned in 3.3.4, the value of the recombination, ionization, trapping and detrapping of equation 2.29 should be zero for a fair test if the mobility is field dependent. This was realized too late in this report to implement and fix, so therefore it is an important aspect to look into. With this, it could be determined fairly accurately if the mobility is field dependent or not.

6.2.4 Using porous media in COMSOL to calculate the processes inside the pressboard

The pressboard in this report has been defined as a solid, which has a specific dielectric constant and a continuous behavior throughout its width. This is a workable simplification of the pressboard, though it will not be able to reproduce all the behavior inside. *Transport of diluted species in Porous media* is a physics that is possible to use through COMSOL. It defines the porosity of the material, the properties of the liquid and the consistency of the solid material. Some effort was put into implementing it into this thesis, however problems occurred regarding the ionization of positive and negative ions. This lead to different results at a point where the results should have been the same. With some work and more understanding of the concept, it is possible to more accurately simulate the processes inside the pressboard.

6.2.5 More in depth analysis of the processes inside the pressboard

The processes inside the pressboard have not been researched thoroughly, which makes a practical thesis to measure and predict the processes inside oil-impregnated pressboard. This could also be performed together with simulation or only simulation itself if more knowledge has been produced by the time the thesis is performed.

6.2.6 Resistivity based on more theoretical analysis

The constant resistivity in this thesis was produced using equations that simplify the calculations and are mostly based on other parameters. Using Onsager's theory, this could be much more in depth about the behavior, how it changes through time and electric field. This part was discussed to be performed in this thesis, but was changed to the field dependency in the different processes in the pressboard.

6.2.7 Improved numerics using a dense mesh and surface charge

As mentioned in section 3.2.3, the mesh of this model was made coarse to get the same spatial resolution as the PEA measurements in [4]. This could be changed into a much denser mesh to improve the results and seeing the real distribution of the space charge density. Using this, it could be useful to compare the COMSOL model with the PEA measurements by integrating the charge density into a surface charge. This should not be too hard to implement, which may disqualify it from a full thesis but be able to be done as a part of a thesis instead.

6.2.8 Implementing a model only dependent on field dependent mobility

In section 3.3.4, it was mentioned that the value of S in equation 2.29 was not zero due to time constraints. Therefore a future work could be to implement that the sum of the trapping, detrapping, recombination and ionization is zero and from there evaluate the field dependent mobility. It may not be enough work for a full thesis, however it might be a good starting point to go further into other subjects.

Bibliography

[1] U. Gäfvert, O. Hjortstam, Y. Serdyuk, C. Törnkvist, and L. Walfridsson, "Modeling and Measurements of Electric Fields in Composite Oil/Cellulose Insulation," in *Conference on Electrical Insulation and Dielectric Phenomena, (CEIDP)*, Kansas City, MO, USA, 2006, pp. 154–157, ISBN: 1-4244-0546-7. DOI: 10.1109/CEIDP.2006.312084. [Online]. Available: https://ieeexplore.ieee.org/document/4105392.

[2] L. Yang, S. Gubanski, Y. V. Serdyuk, and J. Schiessling, "Dielectric properties of transformer oils for HVDC applications," *IEEE Transactions on Dielectrics and Electrical Insulation*, vol. 19, no. 6, pp. 1926–1933, 2012, ISSN: 10709878. DOI: 10.1109/TDEI.2012.6396949.

[3] O. Hjortstam, J. Schiessling, Y. Serdyuk, and S. M. Gubanski, "Measurements of ion mobility in transformer oil: Evaluation in terms of ion drift," in *2012 Annual Report Conference on Electrical Insulation and Dielectric Phenomena*, 2012, pp. 495–498, ISBN: 978-1-4673-1252-3. DOI: 10.1109/CEIDP.2012.6378828. [Online]. Available: https://ieeexplore.ieee.org/document/6378828.

[4] Y. Wu, K. Wu, C. Cheng, *et al.*, "Distinction between the Contributions of Ionized and Injected Charges in Oil Immersed Paper," *IEEE Transactions on Dielectrics and Electrical Insulation*, vol. 28, no. 1, pp. 318–325, Feb. 2021, ISSN: 15584135. DOI: 10.1109/TDEI.2020.009141.

[5] C. Cheng, K. Wu, R. Su, Y. Wu, and J. Dai, "A new method for carrier mobility measurement in oil immersed cellulose paper insulation," *IEEE Transactions on Dielectrics and Electrical Insulation*, vol. 26, no. 1, pp. 308–313, Feb. 2019, ISSN: 15584135. DOI: 10.1109/TDEI.2018.007733.

[6] U. Gäfvert, A. Jaksts, C. Törnkvist, and L. Walfridsson, "Electrical Field Distribution in Transformer Oil," *IEEE Transactions on Electrical Insulation*, vol. 27, no. 3, pp. 647–660, 1992, ISSN: 00189367. DOI: 10.1109/14.142730.

[7] F. Pontiga and A. Castellanos, "Electrical conduction of electrolyte solutions in nonpolar liquids," *IEEE Transactions on Industry Applications*, vol. 32, no. 4, pp. 816–824, 1996, ISSN: 00939994. DOI: 10.1109/28.511637.

[8] L. Onsager, "Deviations from Ohm's law in weak electrolytes," *The Journal of Chemical Physics*, vol. 2, no. 9, pp. 599–615, 1934, ISSN: 00219606. DOI: 10.1063/1.1749541.

[9] K. Giese, "Evaluation of Electrical Tests on Transformerboard," *IEEE Electrical Insulation Magazine*, vol. 9, no. 2, pp. 22–25, 1993, ISSN: 08837554. DOI: 10.1109/57.207265.

[10] I. A. Metwally, "Influence of Solid Insulating Phase on Streaming Electrification of Transformer Oil," Tech. Rep. 3, 1997, p. 327.

[11] R. Liao, J. Hao, G. Chen, Z. Ma, and L. Yang, "A comparative study of physicochemical, dielectric and thermal properties of pressboard insulation impregnated with natural ester and mineral oil," in *IEEE Transactions on Dielectrics and Electrical Insulation*, vol. 18, Oct. 2011, pp. 1626–1637. DOI: 10.1109/TDEI.2011.6032833.

[12] F. Schober, A. Kuchler, W. Exner, C. Krause, and F. Berger, "Influence of board density on the conductivity of oil-impregnated pressboard for HVDC insulation systems," in *33rd Electrical Insulation Conference, EIC 2015*, Institute of Electrical and Electronics Engineers Inc., 2014, pp. 61–64, ISBN: 9781479973521. DOI: 10.1109/ICACACT.2014.7223482.

[13] C. Tang, R. J. Liao, L. J. Yang, and F. L. Huang, "Research on the dielectric properties and breakdown voltage of transformer oil-paper insulation after accelerating thermal ageing," in *2010 International Conference on High Voltage Engineering and Application, ICHVE 2010*, 2010, pp. 389–392, ISBN: 9781424482863. DOI: 10.1109/ICHVE.2010.5640744.

[14] J. Shuo, R. Jiangjun, D. Zhiye, *et al.*, "Charge Transport Simulation in Single-Layer Oil-Paper Insulation," *IEEE Transactions on Magnetics*, vol. 52, no. 3, Mar. 2016, ISSN: 19410069. DOI: 10.1109/TMAG.2015.2469755.

[15] G. Frimpong, U. Gäfvert, and J. Fuhr, "Measurement and Modeling of Dielectric Response of Composite Oil/Paper Insulation," in *Proceedings of 5th International Conference on Properties and Applications of Dielectric Materials*, Seoul, Korea, 1997, pp. 86–89, ISBN: 0-7803-2651-2. DOI: 10.1109/ICPADM.1997.617534.

[16] OECD, "Test No. 301: Ready Biodegradability, OECD Guidelines for the Testing of Chemicals, Section 3," OECD, Tech. Rep., 1992.

[17] Hering VPT, *Hering VPT - Recycling transformer oil*, Sep. 2020. [Online]. Available: https://www.hering-vpt.com/article/recycling-transformer-oil/.

[18] S. Banumathi, T. S. Karthik, M. Sasireka, *et al.*, "Investigation on Dielectric Properties of Press Board Coated with Epoxy Resin, Quartz, and Rice Husk Ash," *Advances in Materials Science and Engineering*, vol. 2021, 2021, ISSN: 16878442. DOI: 10.1155/2021/9839770.